Otoacoustic emissions in humans, birds, lizards, and frogs: Evidence for multiple generation mechanisms

Christopher Bergevin

Speech and Hearing Bioscience and Technology Program
Harvard-Massachusetts Institute of Technology Division of Health Sciences and Technology
Cambridge, MA 02139

Department of Mathematics
University of Arizona
Tucson, AZ 85705
Email: cbergevin@math.arizona.edu
Phone: 520–626–0655
Fax: 520–621–8322

Dennis M. Freeman

Department of Electrical Engineering and Computer Science
Massachusetts Institute of Technology
Cambridge, MA 02139

James C. Saunders

Department of Othorhinolaryngology
University of Pennsylvania
Philadelphia, PA

Christopher A. Shera

Eaton-Peabody Laboratory of Auditory Physiology
Massachusetts Eye & Ear Infirmary
243 Charles Street
Boston, Massachusetts 02114

Department of Otology & Laryngology
Harvard Medical School
Boston, Massachusetts 02115

Abstract

Many non-mammalian ears lack physiological features considered integral to the generation of otoacoustic emissions in mammals, including basilar-membrane traveling waves and hair-cell somatic motility. To help elucidate the mechanisms of emission generation, this study systematically measured and compared evoked emissions in all four classes of tetrapod vertebrates using identical stimulus paradigms. Overall emission levels are largest in the lizard and frog species studied and smallest in the chicken. Emission levels in humans, the only examined species with somatic hair cell motility, were intermediate. Both geckos and frogs exhibit substantially higher levels of high-order intermodulation distortion. Stimulus frequency emission phase-gradient delays are longest in humans but are at least 1 ms in all species. Comparisons between stimulus-frequency emission and distortion-product emission phase gradients for low stimulus levels indicate that representatives from all classes except frogs show evidence for two distinct generation mechanisms analogous to the reflection- and distortion-source (i.e., place- and wave-fixed) mechanisms evident in mammals. Despite morphological differences, the results suggest the role of a scaling-symmetric traveling wave in chicken emission generation, similar to that in mammals, and perhaps some analog in the gecko.

Keywords: OAE, non-mammal, lizard, chicken, frog

Introduction

In both scientific and clinical contexts, evoked otoacoustic emissions (eOAEs) reveal much about the physiology of the ear. However, the actual processes giving rise to emissions remain unclear. Mammalian eOAEs evidently arise from at least two fundamentally different mechanisms (Shera and Guinan 1999). The first mechanism involves induced nonlinear distortion in basilar-membrane (BM) motion, most prominently near the peak of the traveling wave. The second mechanism, described by the theory of coherent reflection (Zweig and Shera 1995), involves "scattering" from pre-existing mechanical irregularities distributed along the cochlear partition.

Models of mammalian eOAEs take specific morphological and functional features of the cochlea into account, such as basilar-membrane traveling waves (Kemp 1986; Zweig and Shera 1995; Talmadge et al. 1998). Furthermore, mammalian hair-cell somatic motility (Brownell et al. 1985) appears necessary to evoke detectable eOAEs using low-level stimuli (Liberman et al. 2004). To match physiological measurements, cochlear models require a region of amplification basal to the peak of the traveling wave (Neely and Kim 1983). The forces responsible for this cochlear amplification are believed to arise from electromechanical transduction in outer-hair-cell soma, although motile responses in the stereociliary bundles may also contribute (Kennedy et al. 2006). The relatively homogeneous morphology of the mammalian cochlea suggests that OAE generation mechanisms are likely to be similar in all mammals.

In contrast to mammals, the non-mammalian vertebrate inner ear exhibits significant anatomical variation across classes (and even species within a given sub-class). Although some features are ubiquitious among vertebrate ears (e.g., stereociliary hair cells), other features, such as hair-cell somatic motility and BM traveling waves, are conspicuously absent in many (if not all) non-mammals. Despite these differences, non-mammals can have relatively low auditory thresholds and sharp tuning. Numerous studies have examined OAEs in representatives of various classes of non-mammals, including lizards (Rosowski et al. 1984; Manley et al. 1993), birds (Taschenberger and Manley 1997), and frogs (van Dijk et al. 1996; Meenderink 2005)[1]. Thus, despite considerable differences in morphology, OAEs appear to be a common feature of vertebrate ears (Köppl 1995). The question therefore arises: Do mechanisms of OAE generation differ between mammalian and non-mammalian tetrapods?

Our purpose here is to systematically compare eOAE properties in order to better understand how and whether generation mechanisms differ across tetrapod classes[2]. Specifically, we address the question: Is there evidence for multiple OAE generation mechanisms in non-mammalian ears? We answer this question by comparing the frequency dependence of eOAE phase for stimulus-frequency emissions (SFOAEs) and distortion-product emissions (DPOAEs), as motivated at the start of the Methods section.

We focus on four different groups: human (*Homo sapiens sapiens*), chicken (*Gallus gallus domesticus*), gecko (two species: *Eublepharis macularius* and *Gekko gecko*), and frog (*Lithobates*

[1]Physiologically vulnerable DPOAEs have also been observed in invertebrates (Coro and Kössl 2001) such as grasshoppers (Kössl and Boyan 1998) and moths (Coro and Kössl 1998).

[2]By generation mechanism we mean the totality of processes that contribute to creating an OAE. Mechanisms encompass the forward propagation path for the evoking stimuli, the production of reverse traveling waves within the inner ear, and the reverse propagation path to the microphone. For example, a mechanism in one species might comprise a mechanical lever (middle ear), a delay line (BM traveling wave), and a group of nonlinear oscillators (hair cells).

pipiens)[3]. These representative species from four different classes display a wide variety of inner-ear morphology, and presumably manifest differences in the way energy propagates through the inner ear and produces tuned responses. For example, the gecko tonotopic map, as determined from auditory-nerve fiber (ANF) responses whose axons were traced back to the BM, goes in the direction opposite of the BM mass gradient (Manley et al. 1999). In other words, the skinny, small end of the gecko BM corresponds to low frequencies and the thick, massive end to high frequencies. This result suggests that ANF tuning in the gecko originates not primarily in the mechanics of the BM but elsewhere [e.g., in the micromechanics of the hair bundle-tectorial membrane complex (Manley et al. 1988; Aranyosi and Freeman 2004)]. Frogs lack a flexible BM altogether, and their hair cells sit directly atop rigid supporting structures (Wever 1985). It has been suggested that traveling waves may still be present in the inner ear of the frog, but on the tectorial membrane (TM) (Hillery and Narins 1984). Furthermore, all the non-mammalian species lack somatic motility in their hair cells (He et al. 2003; Köppl et al. 2004).

Methods

Experimental strategy

This study focuses on the measurement of SFOAEs and cubic DPOAEs ($2f_1 - f_2$ and $2f_2 - f_1$). At low and moderate sound pressures, mammalian SFOAEs and the upper-side-band DPOAE ($2f_2 - f_1$) have rapidly rotating phase-vs-frequency functions. By contrast, the lower-side-band DPOAE ($2f_1 - f_2$) shows almost constant phase when the primary frequencies are swept at near optimal f_2/f_1 ratios. These observations suggest that mammalian SFOAEs and $2f_2 - f_1$ DPOAEs are generated by a mechanism different than that of $2f_1 - f_2$ (Shera and Guinan 1999). Our goal here is to measure these three eOAEs (SFOAE, $2f_1 - f_2$, and $2f_2 - f_1$) in humans, chickens, geckos, and frogs to determine whether and how the emission properties and generation mechanisms compare across this broad range of vertebrate classes. By using a common set of stimulus paradigms and equipment, we hoped to minimize confounding factors when making comparisons across species.

Our strategy for maximizing signal-to-noise ratios while avoiding ambiguities due to the OAE source-type mixing found in mammals (Shera and Guinan 1999) was to use stimulus intensities high enough to produce readily measurable emissions but low enough that phase-gradients and other potentially distinguishing features remained approximately invariant when the stimulus magnitude was lowered further. At first we had no guarantee that such a low-level "linear" regime actually existed in any species save human. Initially, for purposes of mapping out the territory and providing a comprehensive set of inter-species comparisons, we therefore chose to use a common set of low to moderate stimulus intensities in all species. We chose levels of $L_{\rm p} = 40$ dB SPL (SFOAEs) and $L_1 = L_2 = 65$ dB SPL (DPOAEs) and collected the majority of our data using these levels (e.g., Figs. 3–6). In gecko, a group with especially large emission magnitudes, the common stimulus levels proved too high to yield approximately invariant phase gradients, and we therefore also report data measured at lower levels, where phase gradients do not depend strongly on stimulus magnitude. We base our discussion of evidence for multiple emissions mechanisms in gecko on emissions measured using these lower stimulus levels (e.g., Fig. 8).

[3]Frost et al. (2006) have called for a restructuring of the amphibian taxonomy. In their proposed reclassification, leopard frogs are no longer designated as *Rana pipiens pipiens*.

Measurement system

All measurements reported in this study were obtained using the same stimulus paradigms, acquisition codes, and OAE probe for all species/individuals. A desktop computer housed a 24-bit soundcard (Lynx TWO-A, Lynx Studio Technology), whose synchronous input/output was controlled using a custom data-acquisition system. Experiments performed on chicken ears were done at the University of Pennsylvania using a different computer, soundcard (same model) and isolation booth, but all other aspects were identical. A sample rate of 44.1 kHz was used to transduce signals to/from an Etymotic ER-10C (+40 dB gain). The microphone signal was high-pass filtered with a cut-off frequency of 0.41 kHz to minimize the effects of noise.

The probe earphones were calibrated *in-situ* using flat-spectrum, random-phase noise. Calibrations were verified repeatedly throughout the experiment. Re-calibration was performed if the level presented differed by more that 3 dB from the specified value. The microphone calibration was tested using a pistonphone and found to conform well to the shipped specifications. The microphone frequency response was flat (within $\pm$1–2 dB) across the frequency range examined in this study.

Stimulus parameters and analysis

The stimulus frequency range employed ($f_{\rm p}$ for SFOAEs and f_1 for DPOAEs) was typically 0.5–5 kHz for humans, chickens, and geckos and 0.3–3 kHz for frogs. A smaller lower frequency limit was used for some experiments. A suppression paradigm was employed to measure SFOAEs (Brass and Kemp 1993; Shera and Guinan 1999). The suppressor stimulus parameters were as follows: $f_{\rm s} = f_{\rm p} + 40$ Hz, $L_{\rm s} = L_{\rm p} + 15$ dB. One earphone produced a sinusoidal signal over a 464 ms time window at the probe frequency $f_{\rm p}$, ramped on/off over 12 ms at the ends of the window. The other earphone also produced a 464 ms signal, but at the suppressor frequency $f_{\rm s}$, which was ramped on only during the latter half of the window (the first half was silence). The microphone response was extracted from two 186 ms segments from the total waveform, one from the probe alone and one with the probe+suppressor. These segments were extracted at least 20 ms after the end of the ramping-on periods to allow any transient behavior to decay. Thus, the measurements reported here are for the steady-state condition. The Fourier transform of each segment was computed and the complex difference of the two Fourier coefficients at $f_{\rm p}$ was defined to be the SFOAE.

For DPOAEs, each earphone produced a single frequency (f_1 and f_2) over a 244 ms window. Each tone was ramped on and off at the end of the window. A 186 ms segment was extracted from the microphone response. For DPOAE phase measurement, it was necessary to compensate for (electrical) measurement system delays. The corrected DPOAE phase properties for humans compared well with those found in previous reports (e.g., Knight and Kemp 2000).

For both SFOAEs and DPOAEs, 35 waveforms were averaged, excluding any flagged by an artifact-rejection paradigm (Shera and Guinan 1999). Furthermore, all stimulus frequencies were quantized so that an integral number of stimulus periods fit in the response segment. This quantization meant that the nominal values of quantities such as $f_{\rm s} - f_{\rm p}$ and f_2/f_1, which are specified to be constant for a given frequency sweep, varied a small amount between successive steps in a sweep. These variations could be as large as 2%, but typically were much smaller. Frequency step-size during sweeps was small enough to avoid ambiguity during the phase unwrapping. Delays

associated with the measurement system (such as the analog/digital converters on the sound card) were corrected for in the $f_{\rm p}$ phase before taking the complex difference in the SFOAE suppression paradigm.

As indicated for a given figure, error bars indicate the standard error of the mean for a given stimulus condition. The noise floor was defined as the average sound-pressure level centered about (but excluding) the frequency of interest. It was found by averaging the Fourier amplitudes in the ± 3 adjacent frequency bins centered on the OAE frequency. For the stimulus levels used in this study, artifactual system distortion was small compared to the signal levels of the SFOAEs and intermodulation DPOAEs ($\approx$70–80 dB below the evoking stimulus levels and typically beneath the acoustic noise floor). Harmonic system distortion was present (see Fig. 2), but was not characterized for this study.

The phase-gradient delay, as shown in Fig. 8, is computed as the slope of the phase function with respect to frequency. It is given by

$$\tau_{\rm OAE} = -\frac{1}{2\pi}\frac{\partial \phi_{\rm OAE}}{\partial f_{\rm OAE}} \tag{1}$$

where $\phi_{\rm OAE}$ is the emission phase (in radians) and $f_{\rm OAE}$ is the emission frequency [Hz]. The phase-gradient delay is sometimes referred to as the group delay, where it is commonly used in linear systems theory to characterize time delays.

Experimental subjects and animals

Experiments involving humans, geckos, and frogs were all performed at the Massachusetts Institute of Technology. Human experiments were approved by both the Massachusetts Institute of Technology Committee On the Use of Humans as Experimental Subjects and Human-Studies Committee at the Massachusetts Eye and Ear Infirmary. The experimental protocol involving both the geckos and frogs was approved by the Massachusetts Institute of Technology Committee on Animal Care. Experiments involving chickens were performed at the University of Pennsylvania and were approved by the Institutional Animal Care and Use Committee. For all species in this study, OAE data were collected from both males and females and from both ears in a given individual; the results as presented here do not distinguish between sex nor between data collected from left versus right ears.

Human subjects were seated comfortably in a quiet room and were awake for the duration of the experiment. Eight subjects (three males, aged 28, 31, and 64; five females, ages between 26 and 32) with normal hearing participated. Both ears were tested in some, but not all of the subjects. The probe fit snugly into the ear canal using a foam coupling tip.

Nine White Leghorn chickens (*Gallus domesticus*) were used, aged 14–28 days post-hatching and ranging in mass from 150–300 g. The anesthesia paradigm for the chickens was similar to that used in Ipakchi et al. (2003). Briefly, chickens were injected i.m. with urethane (ethyl carbamate) at a dose of 2.5 g/kg. To assure unobstructed breathing, a tracheotomy was performed. Feathers were removed around the external ear opening, but no further surgery was done as a clear path to the tympanic membrane was visible. Chicks were placed on a vibration-isolation table inside a sound-attenuation booth and body temperature was maintained at approximately 41° C via a regulated heating pad. As with the gecko and frog, the probe was coupled to the outer ear via vaseline and a small tube attached to the foam tip. In some cases, the beak was held open using a head-holder

plate, but in others the beak was closed; no systematic differences in emissions between the two conditions were observed. In some experiments, data were obtained from both ears in one animal. Upon termination of the experiment, the chicken was euthanized. Due to respiration and cardiac-related artifacts, the chickens typically exhibited higher acoustic noise floors than the other species (including humans).

For the lizards, nine Leopard geckos (*Eublepharis macularius*) and four Tokay geckos (*Gekko gecko*) were used. Animals were obtained from at least two different vendors for a given species and ranged in mass from 20–55 g (*E. macularius*) and 40–65 g (*G. gecko*). Lizards were kept in aquarium tanks with a 12-hour light cycle and fed crickets dusted with vitamins twice a week. All geckos were healthy and active. Prior to each experiment, an animal was dosed with 25 mg/kg Nembutal i.p. to reduce movement; this dose was effective for approximately four to five hours. The animal recovered completely within a few hours after the experiment and was subsequently used multiple times over the course of two years (always with at least one month recovery time between experiments)[4]. During the experiment, lizards were placed on a vibration isolation table in a noise-reduction chamber. Body temperature is a potential factor that can affect emission properties (see Discussion) and in the case of the lizards, was kept constant by the use of a regulated heating blanket (Harvard Apparatus). Body temperature was monitored using a calibrated thermocouple placed in the mouth, propping it open[5]. Temperature was kept in the range of approximately 27–30° C, depending upon the placement depth of the thermocouple in the mouth. Preliminary experiments indicated that the rate of emission phase accumulation was insensitive to body temperature, though temperature dependence was not thoroughly explored in this study. The probe was coupled to the external ear using a short tube attached to the foam tip and sealed to the head using vaseline. The probe was held in place using a flexible holder. This ensured a tight (closed) acoustic coupling and minimized low-frequency losses.

In the case of the frogs, six leopard frogs (*Lithobates pipiens*) ranging in mass from 40–80 g were used in this study. Emissions were evoked from all ears (except one animal, which failed to produce detectable emissions above the distortion noise floor). Frogs were kept in an aquarium that allowed them to be either in or out of water and were routinely fed vitamin-dusted crickets twice a week. Each frog was given an i.p. injection of Nembutal at a dose of 45 mg/kg. This was sufficient to keep them sedated for five to six hours, after which they recovered completely and were subsequently used in future experiments. The measurement protocol was identical to that for the lizard, except that the heating pad was not used for the frogs. Rather, they were wrapped in wet paper towels to facilitate respiration. As with the gecko, a thermocouple was inserted into the mouth to monitor temperature and had the added effect of propping the mouth open. Body temperature was in the range of 19–21° C and remained relatively stable over the course of the experiment.

[4]For all species where repeated measurements were made in an individual ear during separate experimental sessions, as many as four separate observations may have been made. For data shown in the results section where repeated data from an individual ear is excluded (to avoid bias), the data set that is included was chosen at random. All subjects/animals were healthy to the best of our knowledge during the interval between sessions.

[5]Given the direct coupling between the oral cavity and the middle ear space in non-mammals, OAE measurements could presumably be affected by whether the animal's mouth is open or closed. Provided the calibration was rerun after any changes in the animal's posture, we did not see any evidence over the course of the present study that indicated that emissions are sensitive to whether the animal's mouth is opened or closed. For the sake of consistency, we attempted to make sure the animal's mouth was open for all OAE recordings, though there was some variability in this regard with the chickens.

Results

Individual ears

Figure 1 shows individual SFOAE sweeps from a single representative ear for each group. All groups exhibit emissions whose magnitude varies with frequency. For non-mammals, emissions magnitudes generally become smaller as the frequency increases. Deep notches are apparent in Fig. 1 at irregularly spaced frequencies in both the chicken and gecko, similar to those seen for humans. However, the notches are less numerous than those in the human. Notch frequencies vary from individual to individual within a given species. These notches are highly reproducible in an individual ear during the course of an experimental session, which could last up to three hours. While notches occur reproducibly at certain frequencies across experimental sessions in an individual human, there is some degree of variability in an individual gecko as to whether a particular notch is present and what frequency it occurs at[6]. This inconstancy in an individual gecko ear may be due to seasonal fluctuations or small changes in body temperature. Variability of the magnitude's frequency dependence across sessions for an individual ear was not examined in chickens or frogs. The frog SFOAEs show a magnitude peak near 1 kHz, with magnitudes falling steadily towards the noise floor for frequencies above the peak. This observation is consistent with the notion of the amphibian papilla (AP) being the dominant generator and the basilar papilla (BP) contributing relatively little at these lower stimulus levels (Meenderink and Narins 2006). All groups exhibit significant SFOAE phase accumulation across the frequency range tested (note the different scales in Fig. 1). The rate of phase accumulation decreases with increasing frequency.

Figure 2 shows representative DPOAE spectra for the different groups examined here, using a uniform set of stimulus conditions to facilitate comparison ($L_1 = L_2 = 65$ dB SPL, $f_1 =\sim 1$ kHz and $f_2/f_1 = 1.22$). Intermodulation DPOAEs are present in all species. Numerous higher order distortion products (e.g., $3f_1 - 2f_2$, $5f_2 - 4f_1$) are readily apparent in the gecko and frog ears. For individual DPOAE frequency sweeps, magnitude features for both individual cubic intermodulations are qualitatively similar to those described above for SFOAEs. For example, DPOAE notches occur at specific frequencies that are unique to an individual ear.

Emission magnitude

Figure 3 shows the SFOAE magnitudes compiled from all the individual ears tested for all species[7]. Each point at any given frequency for a particular species represents a unique ear. Only emissions whose magnitude was at least 10 dB above the noise floor are included. Loess trends (locally weighted polynomial regression) are present to guide visualization. To further facilitate comparison, data were pooled into octave bins for a given species and the mean values and 95% confidence intervals are also plotted[8]. Emissions are smallest in the chicken ear and typically largest in the geckos. However, emission magnitudes in the frog ear are also relatively large for $f_{\rm p}$ below ≈ 1.0 kHz, above which they fall off rapidly. Human emission magnitudes are intermediate, except at the

[6] As addressed briefly in the Discussion section, a limited number of experiments were made over the course of the present study where the body temperature of the gecko was varied. The presence of frequency notches was clearly (and reversibly) temperature-dependent.

[7] Figures 3–8 are best viewed in color.

[8] Similar values are obtained when half-octave bins are used.

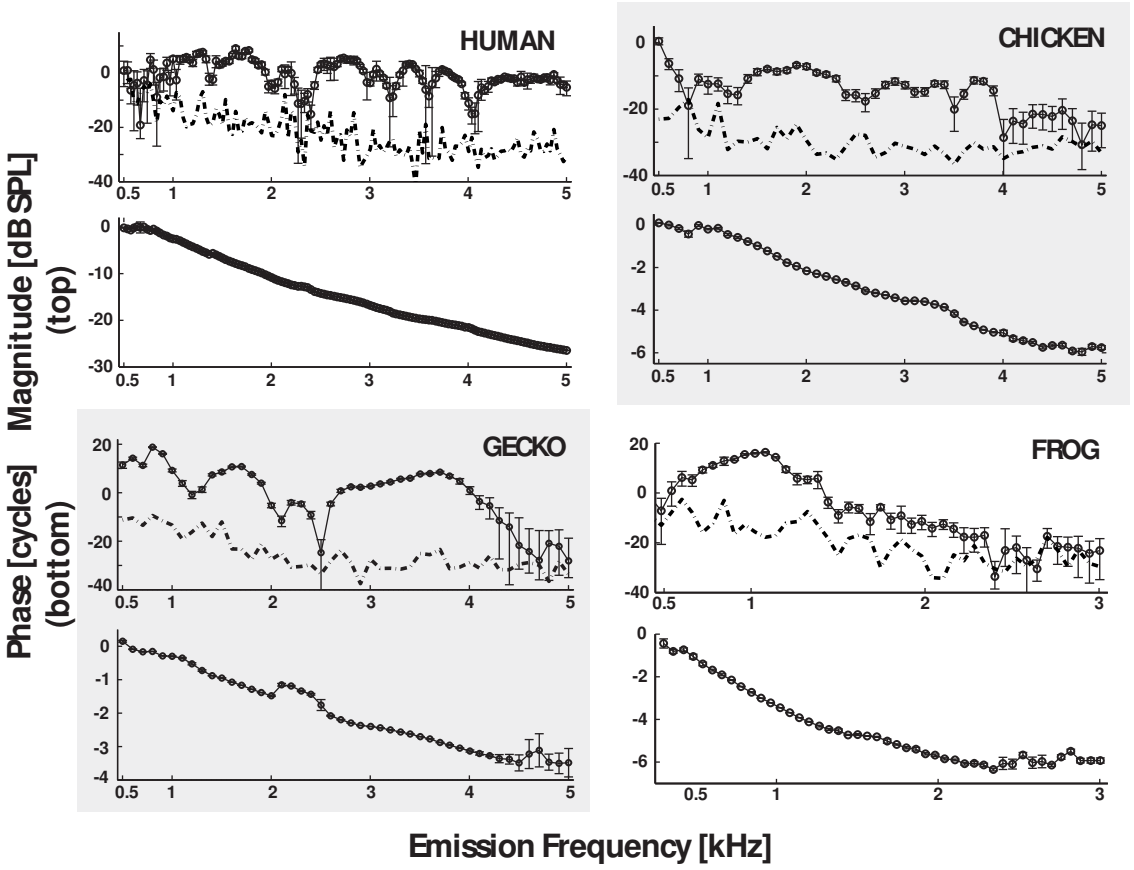

Figure 1: SFOAE sweeps from a representative individual ear from each of the four different groups. Both magnitude (top) and phase (bottom) are shown. Note the different scales across groups. Noise floor is shown by the dashed lines. Error bars indicate standard error of the mean across the 35 measurements taken at a given frequency. [$L_{\mathrm{p}} = 40$ dB SPL, $L_{\mathrm{s}} = L_{\mathrm{p}} + 15$ dB, $f_{\mathrm{s}} = f_{\mathrm{p}} + 40$ Hz]

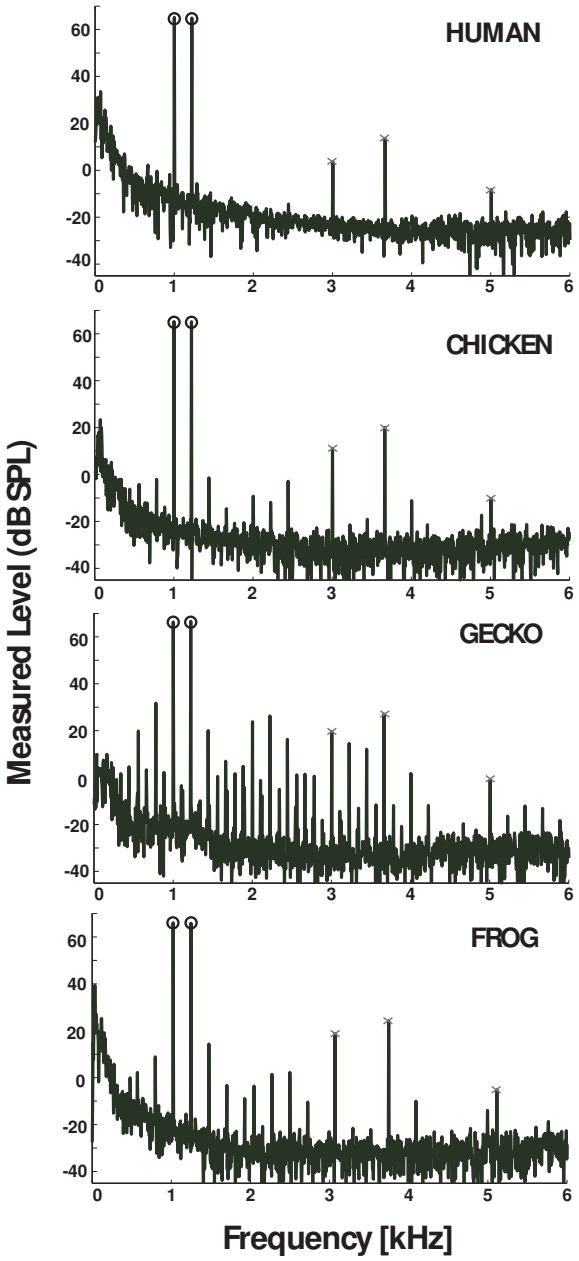

Figure 2: Distortion product spectra from individual ears in four different groups. Stimulus tones are indicated as the spectral peaks with a circle. Harmonic distortion due to the measurement system was not well-characterized and thus DPOAE contribution to harmonic frequencies is unknown (odd-order harmonics are marked by an **x** at the spectral peak). [$L_1 = L_2 = 65$ dB SPL, $f_1 = 1$ kHz (slightly larger for the frog), $f_2/f_1 = 1.22$]

highest frequencies where magnitudes do not decrease to the noise floor as rapidly as the geckos. Emissions in all species are generally largest at lower frequencies (around $\sim$1 kHz) and decrease as stimulus frequency increases.

Figure 4 shows how the average DPOAE magnitudes vary across both species and frequency. For $2f_1 - f_2$, emissions are largest in the gecko for $f_{\rm dp} < 2$ kHz, with *E. macularius* having larger magnitudes than *Gekko gecko*. With the exception of the human and frog, $2f_1 - f_2$ decreases in magnitude with increasing frequency. The frog shows a relatively flat $2f_1 - f_2$ response up to $\sim$1.5 kHz, above which it declines precipitously. The $2f_2 - f_1$ magnitudes are largest in the geckos at all frequencies tested. In humans and chickens, the magnitude of $2f_2 - f_1$ is smaller than that of $2f_1 - f_2$ by $\sim$5–10 dB. At higher frequencies ($f_{\rm dp}$ =2–4 kHz), the $2f_1 - f_2$ magnitude in the human actually increases relative to lower frequencies. For the gecko and frog, $2f_1 - f_2$ is typically smaller than $2f_2 - f_1$ at a given distortion frequency by $\sim$5 dB.

Emission phase

Emission phase is plotted in Fig. 5. This figure shows the unwrapped phase curves measured for all ears tested, including repeats across sessions for the same ear. Relations among the phase curves for humans are consistent with previous reports (Shera and Guinan 1999; Knight and Kemp 2000) and form the basis for the OAE classification criteria described in the introduction. The $2f_1 - f_2$ phase (for fixed f_2/f_1) in humans is relatively independent of frequency above $\sim$ 1.5 kHz while both SFOAE and $2f_2 - f_1$ show significant phase accumulation over the tested range. A qualitatively similar picture is seen in the chicken phase curves. The $2f_1 - f_2$ phase is relatively flat, while the SFOAE and $2f_2 - f_1$ curves have a clear downward trend. Furthermore, a clear difference between the human and chickens is the rate of phase accumulation for both $2f_2 - f_1$ and SFOAE: it is significantly greater in the human.

Both the gecko and frog each exhibit similar amounts of phase accumulation for all three emission types when using moderate stimulus intensities (Fig. 5), in contrast to the human and chicken. Results in both gecko species are similar. The rate of phase accumulation is greater in the frog than the gecko (note the difference in scales for both x and y-axes in Fig. 5).

The rate of phase accumulation was quantified by computing the phase-gradient delay, $\tau_{\rm OAE}$ (see Methods). Both SFOAE and DPOAE phase-gradient delays are shown in Fig. 8. Independent of species and frequency, all SFOAE and $2f_2 - f_1$ delays are $\sim$ 1 ms or longer. Delays are shorter in the chicken and gecko and larger in human and frog. A general feature across groups is that $\tau_{\rm OAE}$ is frequency dependent (see also Fig. 5), delays generally being longer at lower frequencies.

For the human and chicken, $\tau_{2f_1-f_2}$ is small, particularly for emission frequencies above 1.5 kHz. Phase-gradient delays for both $2f_1 - f_2$ and $2f_2 - f_1$ are similar in the frog, when compared at identical emission frequencies. For all species, $\tau_{2f_2-f_1}$ is similar, but not equal, to $\tau_{\rm SFOAE}$ (which is larger by up to a factor of 1.7). The frequency dependence of $\tau_{2f_2-f_1}$ is comparable to that of $\tau_{\rm SFOAE}$.

Dependence of DPOAE phase on primary ratio

As shown by Knight and Kemp (2000), the amount of DPOAE phase accumulation (for fixed ratio f_2/f_1) can have a significant dependence upon the ratio, specifically for $2f_1 - f_2$. In the human ear, the $2f_1 - f_2$ phase is highly frequency dependent at lower ratios (below $\sim$ 1.1), in a manner

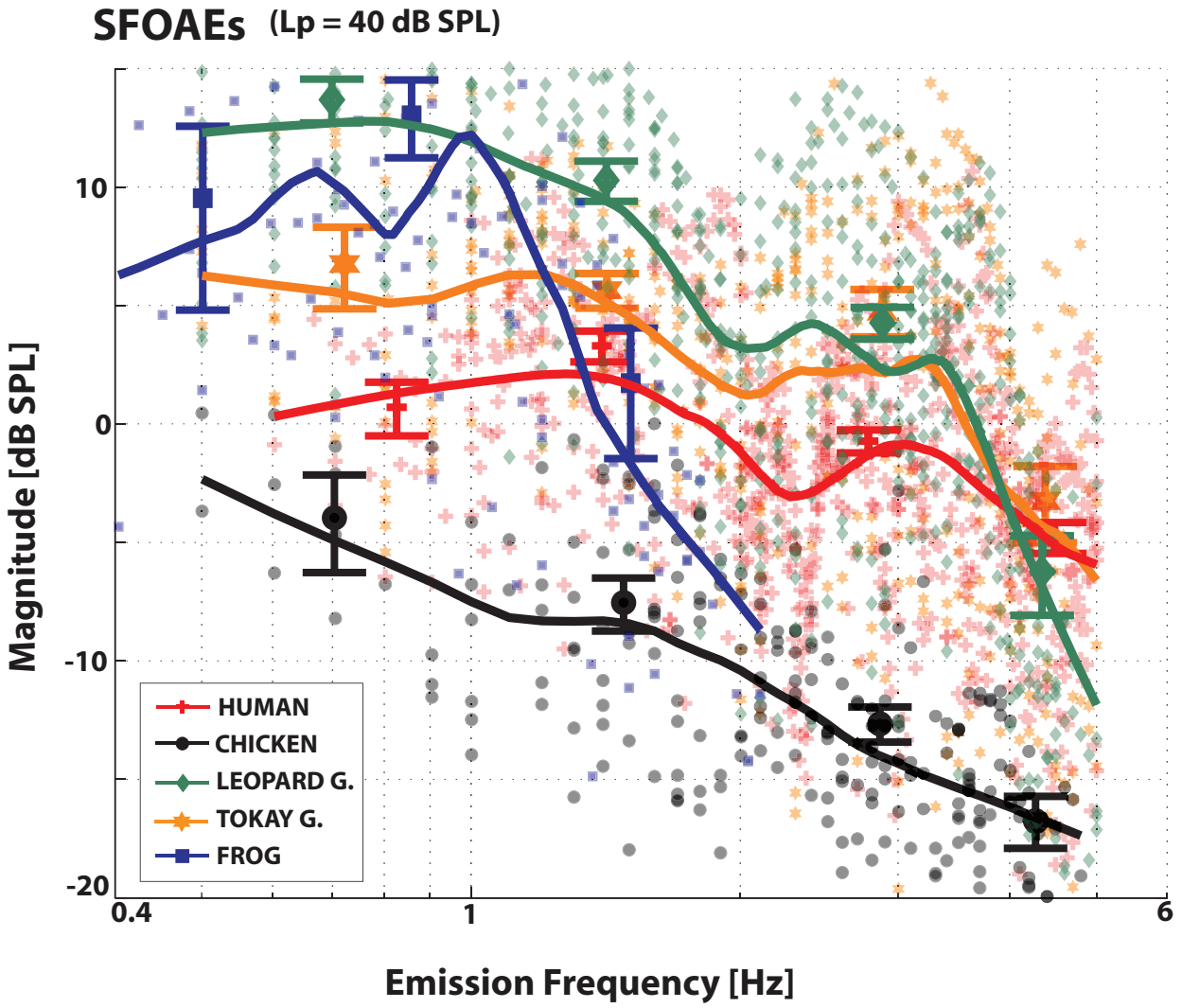

Figure 3: Comparison of SFOAE magnitude across species for $L_{\mathrm{p}} = 40$ dB SPL. The stimulus paradigm used was identical across all species. For any given frequency, each (transparent) data point for a given species/frequency comes from an individual ear. Only points whose magnitude was at least 10 dB above the noise floor are included. Loess trend lines are included to guide visualization. Mean values from octave bins and their 95% confidence intervals are also included.

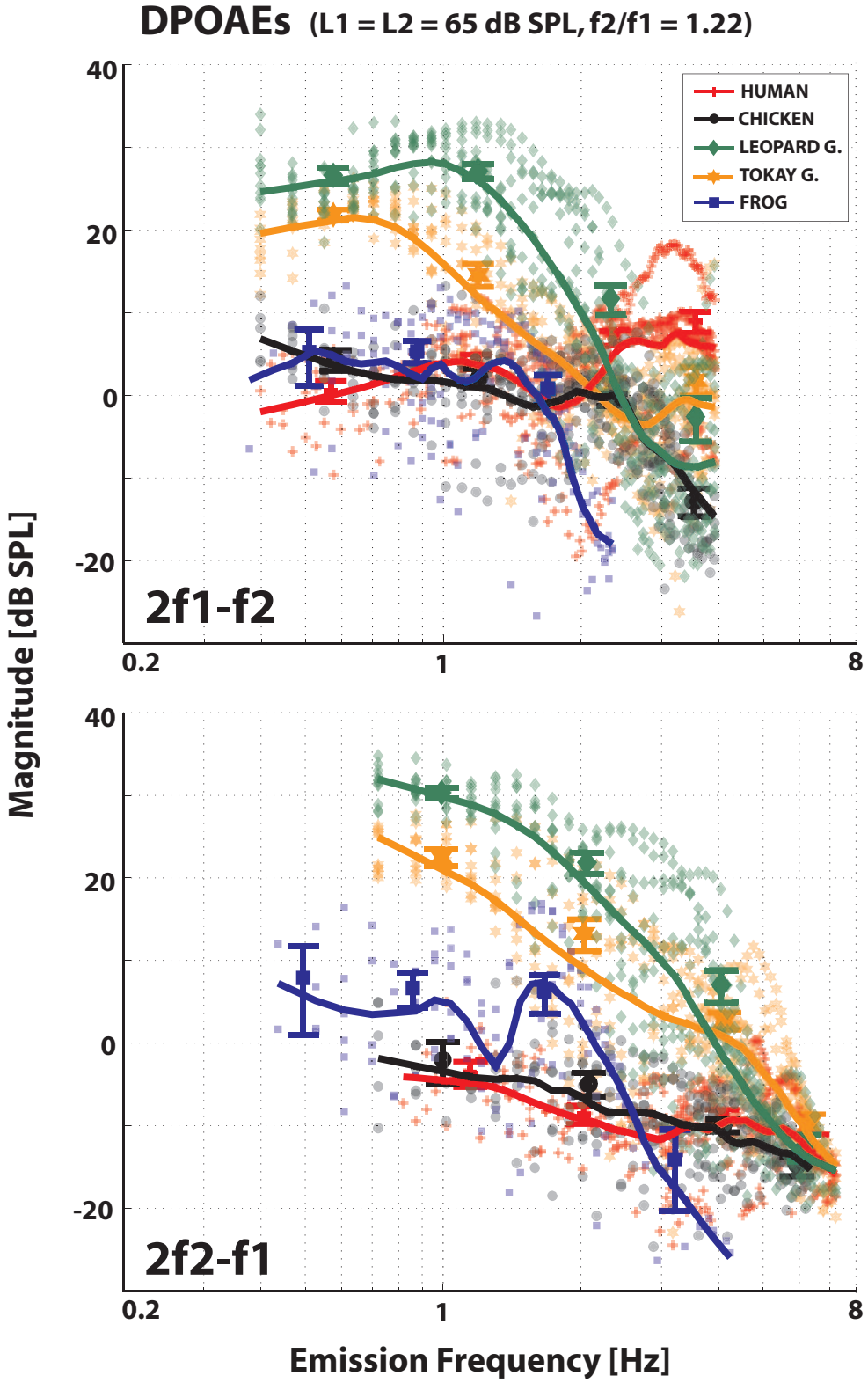

Figure 4: Distortion product magnitude comparison across species for fixed set of stimulus conditions. The low-side $2f_1 - f_2$is on top, while the high-side $2f_2 - f_1$ is on the bottom. Figure structure is similar to that of Fig.3 (i.e. mean values and loess trend lines are indicated in addition to the data points themselves). Only points whose magnitude was at least 10 dB above the noise floor are included. [$L_1 = L_2 = 65$ dB SPL, $f_2/f_1 = 1.22$]

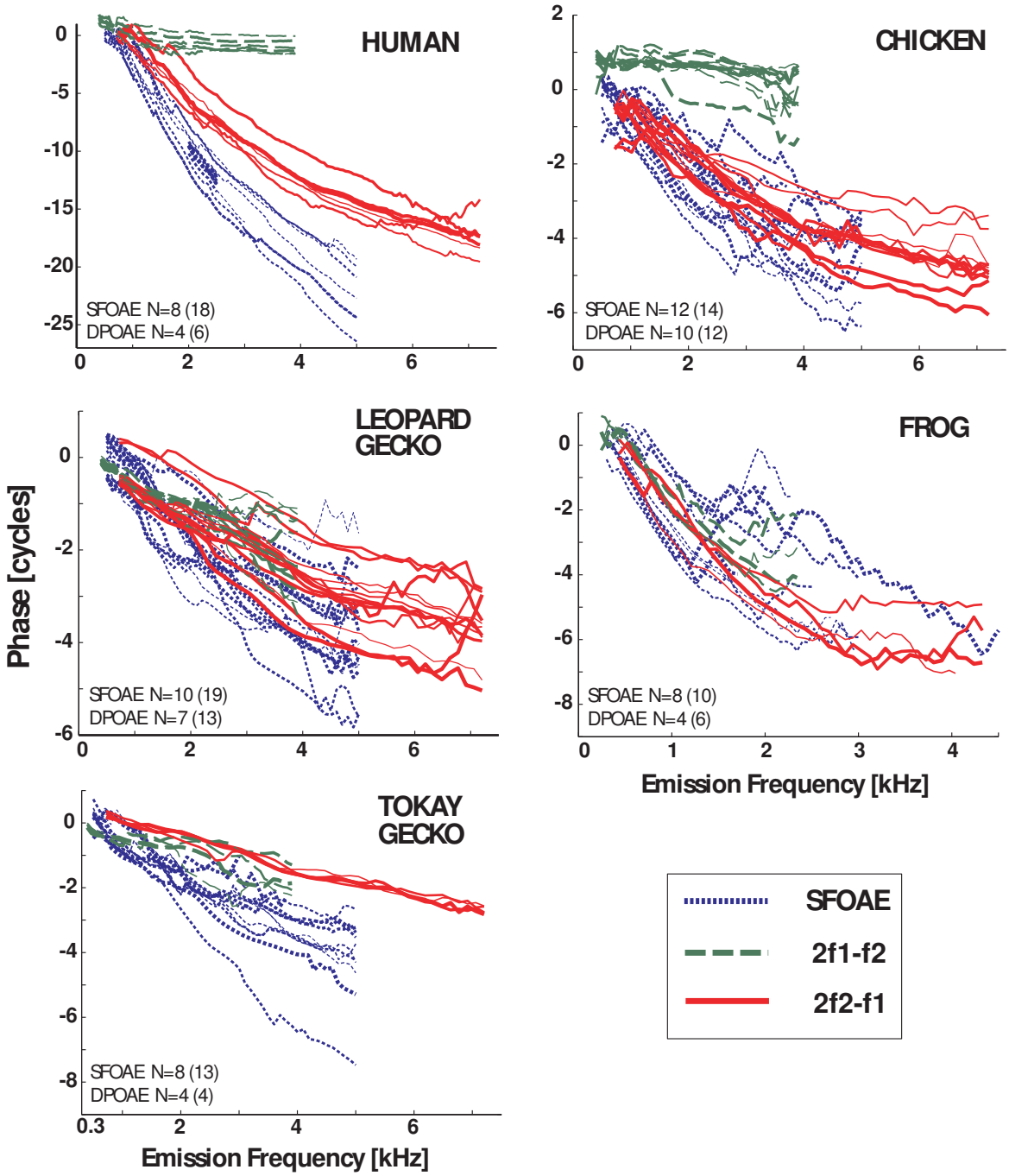

Figure 5: Comparison of emission phase across different OAE types using a common (moderate) stimulus level. Note the different scales across species. For each species, individual curves are plotted using varying line thickness. The total number of unique ears tested is indicated by N. Plots also include repeated measurements in some individual ears at different experimental sessions, as indicated by the number in parentheses which shows the total number of curves plotted. Some phase curves were offset vertically by an integral number of cycles for clarity. [SFOAE: $L_\mathrm{p} = 40$ dB SPL, $L_\mathrm{s} = 55$ dB, $f_\mathrm{s} = f_\mathrm{p} + 40$ Hz, DPOAE: $L_1 = L_2 = 65$ dB SPL, $f_2/f_1 = 1.22$.]

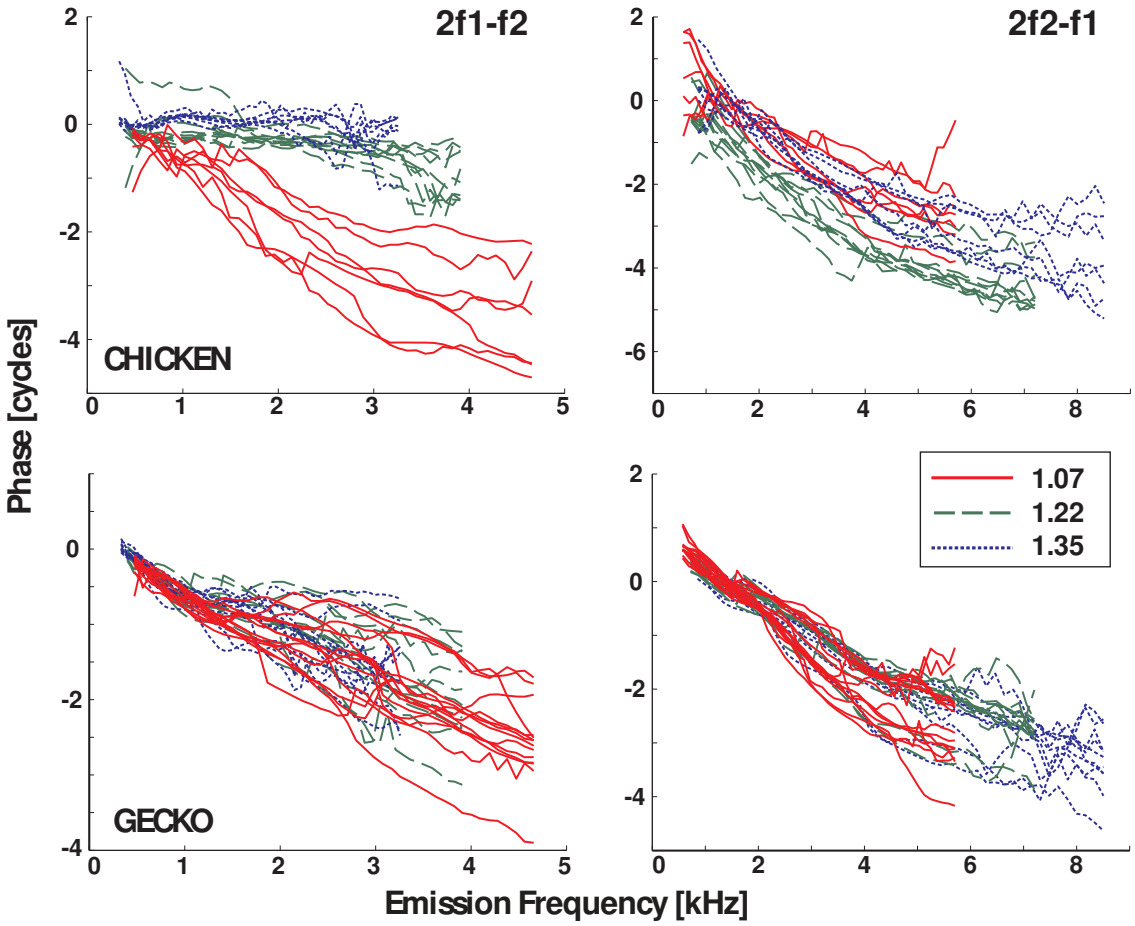

Figure 6: Distortion-product phase dependence upon primary ratio at moderate stimulus levels in both chicken (top row) and gecko (bottom row). Both gecko species are pooled together. For a given group, each curve represents an individual ear. For any given ear, both $2f_1 - f_2$ (left column) and $2f_2 - f_1$ (right column) were measured simultaneously. [$L_1 = L_2 = 65$ dB SPL, $f_1 = 0.5$–5 kHz in 0.1 kHz steps.]

similar to that of the SFOAE and $2f_2 - f_1$ phase curves. Around $f_2/f_1 \sim 1.1$, there is a sharp transition where the $2f_1 - f_2$ phase becomes frequency-independent. $2f_2 - f_1$ phase behavior is relatively insensitive to the primary ratio in humans.

Figure 6 shows how DPOAE phase gradients depend upon primary ratio in non-mammals. Chicken results are qualitatively similar to those seen in humans. The $2f_1 - f_2$ phase shows significant phase accumulation at smaller ratios while very little at higher ratios. Also similar to humans, the transition for chickens occurs around $f_2/f_1 \approx 1.09 - 1.1$. The result is quite different in the gecko ear (both species are pooled together in Fig. 6), where both cubic DPOAE phase curves are comparatively insensitive to primary ratio. Results in the frog (not shown) are similar to those of the gecko in that the DPOAE phase gradients are also invariant with respect to primary ratio and $2f_1 - f_2$ does not appear to flatten out.

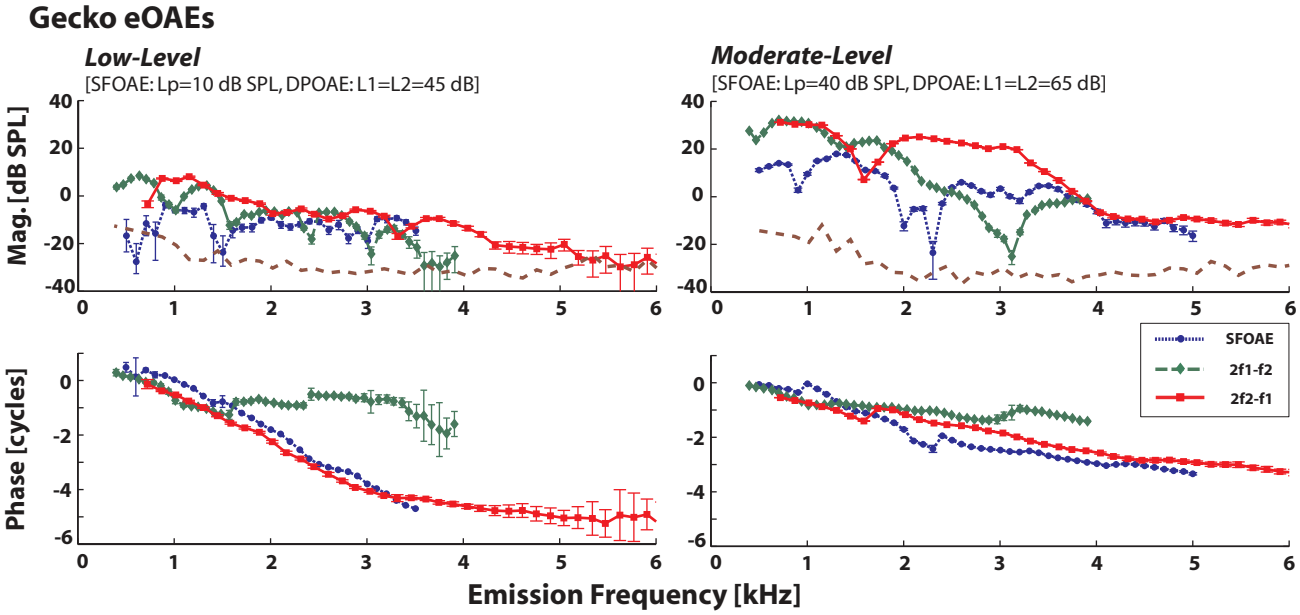

Figure 7: Comparison of SFOAEs and DPOAEs evoked using both low (left) and moderate (right) stimulus levels in an individual *E. macularius* ear. Similar behavior was seen in the majority of other geckos. [**SFOAEs:** $L_\mathrm{p} = [10, 40]$ dB SPL, $L_\mathrm{s} = [35, 55]$ dB, $f_\mathrm{s} = f_\mathrm{p} + 40$ Hz **DPOAEs:** $L_1 = L_2 = [45, 65]$ dB SPL, $f_2/f_1 = 1.22$.]

Dependence on stimulus magnitude

Emission phase behavior depends upon stimulus magnitude. Figure 7 shows DPOAE and SFOAE phase curves from an individual *E. macularius* evoked using both lower stimulus intensities [left: $L_\mathrm{p} = 10$ dB SPL for SFOAEs and $L_1 = L_2 = 45$ dB SPL for DPOAEs] and moderate stimulus levels (right side: levels were same as those used in Figs. 1–5). The low-level phase behavior in this gecko appears qualitatively similar to that seen in the human and chicken; in particular, $2f_1 - f_2$ exhibits significantly less phase accumulation than either the SFOAE or $2f_2 - f_1$. While the dependence upon stimulus magnitude was not systematically explored across species in this study, measurements at lower levels in several geckos (both species) revealed behavior similar to that in Fig. 7. This similarity in the phase behavior between the gecko (at low levels) and humans/chickens (at moderate levels) can be seen in the phase-gradient delays (Fig. 8). No deviations from the general phase trends shown in Fig. 5 were observed in the frog, even at lower stimulus intensities. Specifically, both cubic DPOAE phase curves for a given frequency sweep had similar amounts of phase accumulation in the frog[9]. Furthermore, the level-dependence of SFOAE phase gradients in the gecko appears qualitatively similar to that previously reported for humans (Schairer et al. 2006): in both species the gradients become shallower at higher stimulus levels with a transition between the two regimes beginning at probe levels around 40 dB SPL (data not shown).

[9]Measurements of DPOAEs in several frogs using a fixed f_2/f_1 ratio of 1.22 and stimulus intensities ($L_1 = L_2$) ranging from 45 to 75 dB SPL provided no indication that the $2f_1 - f_2$ phase flattens out relative to that of $2f_2 - f_1$ or the SFOAE (although phase gradients for a given OAE did vary some with level). DPOAEs at primary levels below 65 dB SPL for ratios other than 1.22 were not measured in this study for the frog.

Discussion

Low to moderate stimulus magnitudes generated measurable SFOAEs and DPOAEs in all tetrapod classes examined. After briefly reviewing methodological issues that can complicate inter-species comparisons, we discuss emission similarities and differences with regard to the morphological and physiological variations in the auditory periphery across species. In particular, we will address differences in emission phase behavior and provide an interpretation within the context of generation mechanisms.

Methodological and other issues

Comparison to previous studies

When comparisons are possible, our results are generally consistent with previous reports. One confounding factor is stimulus magnitude: the present results were obtained using stimulus levels that were typically lower than those employed in previous studies, making direct comparison difficult. Another factor is that many previous studies of non-mammalian eOAEs did not report phase-gradient delays.

For humans, both the DPOAEs and SFOAEs magnitudes and phase-gradient delays are similar to those described in the literature (Knight and Kemp 2000; Schairer et al. 2006). Distortion product magnitudes at $2f_1 - f_2$ in the chicken ear (Kettembeil et al. 1995; Ipakchi et al. 2005; Lichtenhan et al. 2005) show some differences across studies (approximately ± 7 dB difference in magnitudes). One key difference across chicken studies is the type of anesthesia used, as addressed in the next section. SFOAEs have been reported in avian ears (Manley et al. 1987), but differences in measurement paradigms and species make them difficult to compare directly with ours. Although DPOAEs have been measured in a number of lizard species (e.g., Rosowski et al. 1984; Manley et al. 1993), we know of no reports specifically in the gecko. Nevertheless, our gecko DPOAEs appear qualitatively consistent with those in other lizard species. With respect to the frogs, both SFOAEs (Meenderink and Narins 2006) and DPOAEs (Meenderink et al. 2005) were examined in the same species used here. Although overall trends with frequency are similar, previous DPOAE magnitudes are typically 5–15 dB smaller than those reported here. The reason for this difference is unclear. While the phase-gradient delays in the frog ear are similar across studies, the values reported here tend to be larger for $2f_1 - f_2$ (particularly at lower frequencies) and for SFOAEs, possibly as a result of the lower stimulus levels employed in the present study.

Anesthesia

In the present study, all species except the human were anesthetized. In principle, the depth and type of anesthesia can influence comparisons across species. Although we did not systematically examine the influence of anesthesia on eOAEs, previous studies are consistent with our own informal observations indicating that anesthesia has a relatively minor effect on eOAE magnitudes evoked via a low-level stimulus. We know of no studies looking at the effect of anesthesia upon human eOAEs, but results from guinea pig (Boyev et al. 2002) and rabbits (Martin et al. 1999) have indicated that anesthesia either has no effect or causes a slight reduction in DPOAE magnitudes when no efferent contributions are involved. In the chicken, Kettembeil et al. (1995) re-

ported that emission magnitudes decline and eventually fall below the noise floor as the depth of anesthetization increases. Although our chickens were deeply anesthetized, the similarity in emission magnitudes relative to the results reported by Kettembeil et al. (1995) (whose chickens were awake) suggests that anesthesia did not significantly affect the emission generation mechanisms in chickens. Our own observations indicate that the depth of anesthesia has some effect upon gecko DPOAEs at high emission frequencies (2-3 kHz), emissions being slightly smaller in the more deeply anesthetized state. Taken together, these results suggest that for low to moderate stimulus intensities, if anesthesia has any effect at all, it is to decrease emission magnitudes.

The effect of anesthesia upon emission phase is less clear. How anesthesia affects phase-gradient delays in humans, chickens, and frogs was not examined in the present study and remains unknown. Informal observations in two geckos suggest that depth of anesthesia had no systematic effect upon emission phase. Although further study is needed, the results from the gecko suggest that anesthesia is unlikely to be a major confounding factor when comparing emission phase behavior across species.

Body temperature

Another important factor when comparing emissions across species is body temperature. In this study, the goal was to keep the individuals of a given species at a uniform body temperature close to their preferred native thermal condition. For the chickens and geckos we used a heating pad or blanket. For all the non-mammalian species, the chosen body temperature was believed to correspond to that at which emission magnitudes were approximately maximal.

In humans, emission magnitudes have been reported to decrease when body temperature is either decreased (Veuillet et al. 1997) or increased (Ferber-Viart et al. 1995) from its normal value [37° C]. To the best of our knowledge the effect of temperature upon avian eOAEs has not been examined. However, pigeon ANF responses have been found to shift their CF with temperature and become less sensitive as temperature is decreased below normal (Manley 1990). Furthermore, SOAEs in the barn owl systematically shift in frequency as body temperature is varied, although their magnitudes remain relatively constant (Taschenberger and Manley 1997). Frog DPOAE magnitudes appear fairly insensitive to temperature, though emission magnitudes at lower frequencies/stimulus levels were found to decrease when body temperatures dipped below ∼19° C (Meenderink and van Dijk 2006).

The authors know of no reports on the temperature dependence of eOAEs in lizards. Lizard SOAEs (including those from gecko) are temperature-dependent, but only with regard to emission frequency (higher temperature shifts the frequency upward) (Manley and Köppl 1994; Manley et al. 1996). SOAE magnitude appears little affected by body temperature, except at extreme deviations (Manley et al. 1996). Werner (1976) remarked that the "optimal temperature range" for cochlear potential threshold in *Eublepharis macularius* is 30–40° C and 25–30° C in *Gekko gecko*, also noting that these ranges correspond the gecko's ecologically preferred temperature range. We performed a limited number of experiments in which the temperature was decreased and subsequently raised (range of ∼18–29° C). The results indicate that gecko eOAEs tend to be larger in the higher temperature regime (∼30° C), particularly at higher frequencies and when using lower level stimuli.

The effect of temperature upon the frequency dependence of emission phase has not been examined in human, chicken, or frog. In gecko, observations made during the present study suggest

that body temperature can have a small effect upon phase-gradient delays. At lower body temperatures ($\sim$18° C), both SFOAE and DPOAE delays were slightly smaller than those at higher temperatures for emission frequencies around 1.5–3 kHz. Above $\sim$22° C, temperature appears to have little effect upon the emission phase in the gecko.

Stimulus magnitude

In humans and other mammals, evidence for multiple emission source types comes from eOAE phase gradients measured at low and moderate stimulus levels. At higher levels, all eOAE phase gradients become shallower (Whitehead et al. 1996; Schairer et al. 2006; Long and Talmadge 2007) and the clear difference between the SFOAE and $2f_1 - f_2$ phase gradients largely disappears, perhaps because of source-type mixing (Shera and Guinan 1999, Talmadge et al. 2000, Goodman et al. 2003). Our goal in chickens, geckos, and frogs was to measure emission phase gradients at levels low enough such that decreasing the magnitude did not qualitatively change the observed phase behavior. Of course, we had no guarantee at the outset that a linear "low-level" regime analogous to that seen in humans would actually exists in the other species[10]. Our results, however, establish that such a regime does exist in all non-mammalian species examined, although its approximate upper magnitude limit appears variable. For example, although DPOAE primary levels of 65 dB SPL were adequate in humans and chickens, substantially lower intensities (around 45 dB SPL) proved necessary in the gecko. We speculate that the lower stimulus levels needed in gecko reflect the substantially higher overall level of distortion found in this group; as a result of the increased distortion, contamination by source-type mixing presumably occurs at lower stimulus intensities than in humans.

Species differences in emission magnitude

In the non-mammals, emission magnitudes fall into the noise at stimulus frequencies that correlate well with the approximate upper limits of hearing determined from auditory threshold curves (Manley 1990; Ronken 1991) (see Figs. 3 and 4). The correlated increase in hearing thresholds and decrease in emissions could be due to poor high-frequency middle-ear transmission and/or to the absence of hair cells responsive to high frequencies (Manley 1990). In the frog, our observation that eOAE magnitudes fall off rapidly above ~ 1 kHz appears consistent with previous suggestions that the two papillae act as separate emission sources with different sensitivities (Meenderink et al. 2005). In the species of frog examined here, the AP is most sensitive to frequencies below ~ 1.3 kHz (Ronken 1991). The single peak in the frog SFOAE magnitude spectrum (Fig. 3) contrasts with the twin peaks found in previous studies (Meenderink and Narins 2006). This disparity between the studies can be explained by the observation that higher levels than those used here are required to evoke measurable emissions from the BP (Meenderink et al. 2005). The low-frequency SFOAEs reported here presumably come primarily from the AP.

For moderate level stimuli, and at frequencies within their range of hearing, DPOAE and SFOAE magnitudes are clearly largest in gecko and frog (Figs.3 and 4). Interestingly, the two

[10]Based upon differences in the DPOAE physiological vulnerability in the frog ear, van Dijk et al. (2003) indicated a distinction between low and high-level emissions. Their distinction is different however than the one we make here: we are primarily concerned with the linearity of the OAE response. How the distinctions between low and high-level emission generation mechanisms made here and that made by van Dijk et al. are related is not presently clear.

groups with the largest emission magnitudes are the ones who lack a tuned basilar membrane, have the fewest total number of hair cells, and manifest no somatic hair-cell electromotility. Evidently, morphological and functional features of the mammalian cochlea thought to play important roles in OAE generation are neither necessary for generating OAEs nor needed for producing large ones.

Four broad classes of explanations for the larger emission magnitudes in gecko and frog come to mind, none of them mutually exclusive. First, forward and reverse middle-ear transmission may be more efficient in these species. Second, the evoking stimuli and/or the emissions themselves may undergo greater enhancement as they travel to and from the sites of emission generation within the inner ear. Third, at moderate stimulus intensities the emission "sources" (e.g., inner-ear nonlinearities) may be intrinsically stronger in the gecko and frog. This explanation appears consistent with the large number of high-order distortion products measurable in these species (see Fig. 2). Finally, the absence of a tuned BM may reduce or eliminate the emission filtering or phase cancellation effects believed to occur in the mammalian cochlea (e.g., Shera 2003; Shera and Guinan 2007). This explanation is consistent with the approximate symmetry between lower- and upper-side-band DPOAEs observed in these species. In mammals, by contrast, upper-side-band DPs (e.g., at $2f_2 - f_1$) that arise in the the primary overlap region near the f_2 place are produced in the non-propagating region apical to their best place. As a result, the corresponding DPOAE magnitudes are reduced.

Species differences in emission phase gradients

Emission phase gradients reveal information about the mechanisms of emission generation (Brown and Kemp 1983; Shera and Guinan 1999). In mammalian ears, two broad classes of generation mechanisms—wave-fixed and place-fixed—have been identified. The appropriate classification can often be inferred from the relative size of the emission phase gradient. Shallow phase gradients—interpreted using the local scaling symmetry[11] of mammalian mechanical responses—imply that the dominant emission sources are induced by the response to the stimulus. An example would be the nonlinear distortion that occurs when primary traveling waves interact to produce distortion products. Because induced sources move with the stimulus envelope when the frequencies are varied, they are known as wave-fixed. By constrast, rapidly rotating emission phases imply that emission generation involves processes that violate local scaling. An example here would be scattering off pre-existing perturbations or generation by other sources that are fixed in space (place-fixed). Note that although the "wave-fixed" nomenclature originates from the study of mammalian OAEs, where responses to stimuli take the form of BM traveling waves, the concept does not require waves, per se. For the purposes of generalizing across species, a better name might be "stimulus-induced."

Table I provides a brief summary of the emission phase behavior observed in the four groups at low stimulus intensities. The summary is based on Fig. 5 (for human, chicken, frog) and on Fig. 7 (for gecko). The table classifies the overall phase gradients as either "steep" ($\searrow$, suggesting a place-fixed mechanism) or "shallow" ($\longrightarrow$, suggesting a stimulus-induced mechanism) for each

[11]Within the context of cochlear traveling waves, local scaling implies that the number of wavelengths (i.e., the total amount of phase accumulation) between the stapes and the peak of the traveling wave varies only slowly with frequency.

	Human	Chicken	Gecko	Frog
SFOAE	$\searrow$	$\searrow$	$\searrow$	$\searrow$
$2f_2 - f_1$	$\searrow$	$\searrow$	$\searrow$	$\searrow$
$2f_1 - f_2$	$\longrightarrow$	$\longrightarrow$	$\longrightarrow$	$\searrow$

Table I: Capsule summary of the frequency dependence of emission phase at low stimulus intensities drawn from Fig. 5 (for human, chicken, frog) and from Fig. 7 (for gecko). The symbol $\searrow$ indicates a steep phase curve; the symbol $\longrightarrow$ a shallow one.

OAE type (SFOAEs and $2f_1 - f_2$ and $2f_2 - f_1$ DPOAEs). Figure 8 shows quantitative values of the OAE phase-gradient delays across frequency for each of the four groups. As Fig. 8 makes clear, phase-gradient delays vary considerably in overall size between groups. The terms "steep" and "shallow" are therefore relative terms more meaningfully applied within rather than across groups. With the generalizations provided by Table II as a rough guide, we now discuss and interpret the data for each group in turn.

Humans and other mammals

Consistent with earlier reports in humans (e.g., Shera and Guinan 1999; Knight and Kemp 2000), we find that $2f_1 - f_2$ DPOAE phase gradients are close to zero (i.e. phase-versus-frequency functions are almost constant) when measured using primary tones swept at near optimal frequency ratios ($f_2/f_1 > 1.1$) at f_2 frequencies greater than 1–1.5 kHz. Similar results are found in the basal turns of other mammals, suggesting that these DPOAEs originate via wave-induced sources. By contrast, both SFOAEs and upper-side-band DPOAEs ($2f_2 - f_1$) have steep phase gradients (rapidly rotating phases), suggesting that these emissions arise by place-fixed mechanisms. Nearly constant at f_2 frequencies above 1 kHz, $2f_1 - f_2$ phase gradients increase somewhat in the apical half of the cochlea, but remain significantly smaller than the gradients characteristic of SFOAEs and $2f_2 - f_1$ DPOAEs. This apical increase in the $2f_1 - f_2$ phase gradient may reflect violations of scaling in the apex (e.g., van der Heijden and Joris 2006) or perhaps a transistion to more place-fixed generation. In summary, both wave- and place-fixed mechanisms for OAE generation operate in the mammalian ear.

Chickens

Phase gradients from the chicken appear qualitatively similar to those of the human. As in mammals, the $2f_1 - f_2$ DPOAE phase is almost constant and both the SFOAE and the $2f_2 - f_1$ DPOAE manifest a significant rate of phase accumulation (Fig. 5). The phase slope is, however, substantially less than that in humans. As in humans, the near identity of the $2f_2 - f_1$ and SFOAE gradients suggests that these two emissions are generated by similar mechanisms. Furthermore, the near constancy of the $2f_1 - f_2$ DPOAE phase suggests that mechanical responses in the chicken manifest an analogue of the local scaling symmetry observed in the mammal. This otoacoustic evidence for scaling-symmetric responses in the avian ear is consistent with mechanical measurements (von Bekesy 1960; Gummer et al. 1987). Additional resemblances between humans and chicken DPOAEs include a similar dependence of DPOAE phase on primary ratio (Fig. 6; Knight and Kemp 2000). Although chickens lack somatic electromotility, their OAEs manifest many similarities to those of mammals, including evidence for both wave- and place-fixed sources.

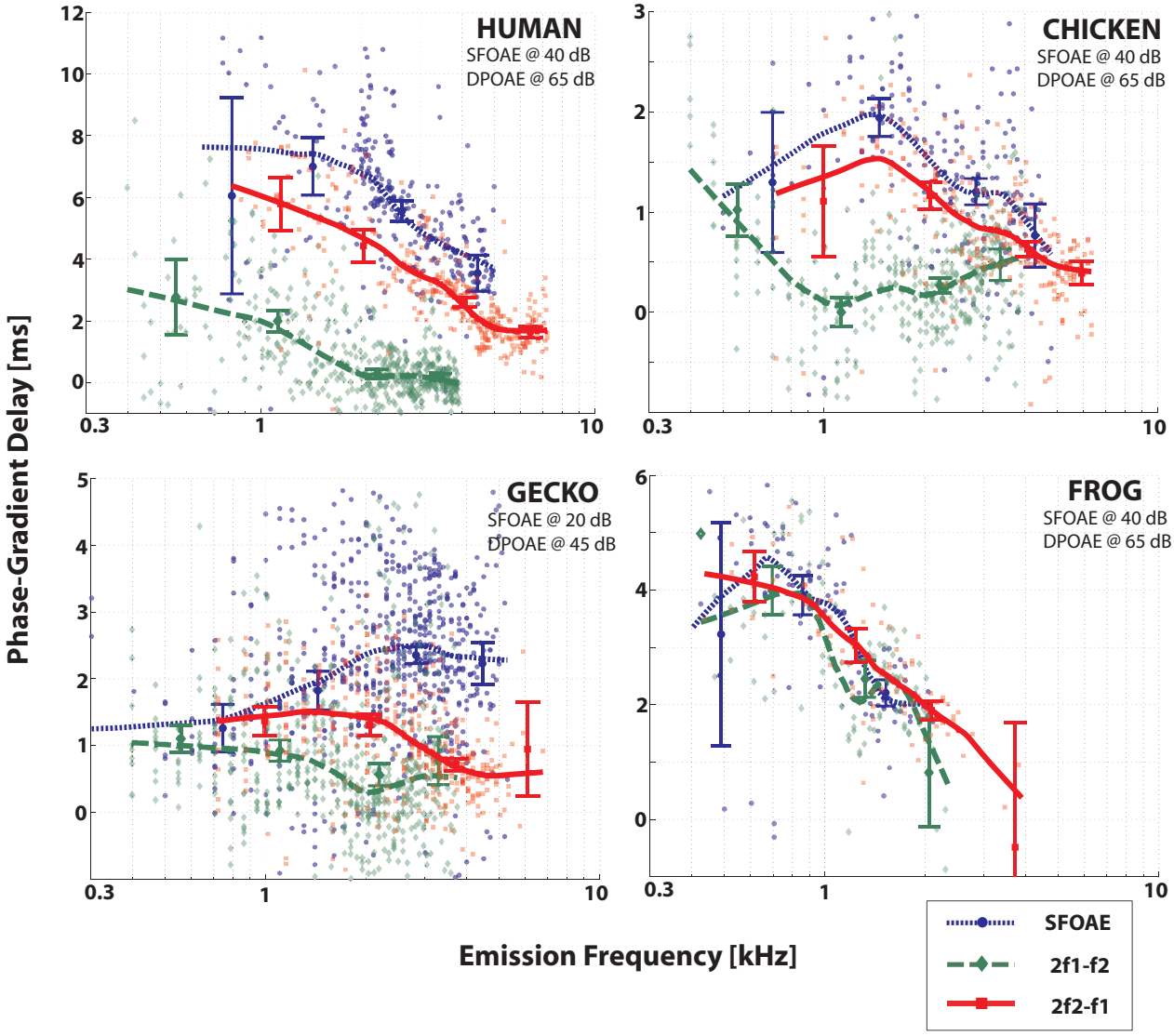

Figure 8: Phase-gradient delays [ms] for all three emission types. Both gecko species are grouped together here. Individual data points are included as well as loess trend lines. Furthermore, data were also lumped into octave bins and the mean and 95% confidence intervals are also indicated (plotted against the geometric mean frequency). [**SFOAEs:** $L_\mathrm{p} = 40$ dB SPL, $L_\mathrm{s} = 55$ dB, $f_\mathrm{s} = f_\mathrm{p} + 40$ Hz for human, chicken and frog, $L_\mathrm{p} = 20$ dB SPL, $L_\mathrm{s} = 35$ dB for the gecko; **DPOAEs:** $L_1 = L_2 = 65$ dB SPL, $f_2/f_1 = 1.22$ for human chicken and frog, $L_1 = L_2 = 45$ dB SPL for the gecko.]

Geckos

Differences between SFOAE and $2f_1 - f_2$ phase-gradient delays consistent with those seen in mammals and chickens are also evident above 1 kHz in the gecko (Fig. 8). Recall, however, that we needed to employ lower stimulus intensities in the gecko before the differences in DPOAE phase gradients became apparent (Fig. 7). Above 1 kHz, $2f_2 - f_1$ phase gradients are relatively smaller than those of the SFOAEs than they are in the other species. Nevertheless, the differences between SFOAE and $2f_1 - f_2$ gradients at low levels suggests an analog of the wave- and place-fixed distinction operating in mammals (and chickens). Below 1 kHz, all three gradients have similar values and provide no evidence for multiple mechanisms. In addition, we found that below 1 kHz, SFOAE phase-gradient delays vary signficantly less with probe level than they do above 1 kHz. Interestingly, the 1 kHz boundary between "low-" and "high-frequency" OAE behavior correlates well with the CF near the morphological transition between the basal continuous TM (uni-directional) region and the more apical bi-directional region (see Fig. 1), as determined using ANF-tracing (Manley et al. 1999). The overlying tectorial topology is also different in these two regions (a basal TM meshwork versus an apical sallets/continuous smooth TM). Whether and how these morphological differences contribute to the functional differences we measured via OAEs remains an outstanding question.

Frogs

Unlike the phase-gradient delays in the three other groups, those in frog provide no evidence for multiple generation mechanisms. The SFOAE, $2f_1 - f_2$, and $2f_2 - f_1$ delays appear similar (Fig. 8) at all frequencies, intensities, and primary ratios examined. Below 1.5–2 kHz phase-gradient delays in the frog are significantly longer than those in gecko and chicken but shorter than those in human (except for $2f_1 - f_2$).

Our results do not preclude the possibility of a traveling wave playing some role in OAE generation in the frog ear, in spite of the absence of a flexible BM. Since the mammalian tectorial membrane supports wave-like behavior (Ghaffari et al. 2007), the tectorial curtain provides an obvious potential source of a traveling-wave like delay in the frog [as suggested by Hillery and Narins (1984)][12]. A naive interpretation of the present results is that the long delays in frogs appear consistent with the predominance of place-fixed generation mechanisms. The absence of evidence for a wave-fixed mechanism could be explained by a number of different factors. In mammals, the shallow phase gradients characteristic of $2f_1 - f_2$ at optimal ratios require three things: (1) OAE generation via induced sources, (2) approximate local scaling symmetry, and (3) the absence of other significant sources of delay (e.g., long transmission delays through the middle ear). Thus, wave-fixed behavior can be masked experimentally by the absence of scaling or the presence of additional delays.

[12] A mechanical delay stemming from a traveling wave in the TM of the AP could explain the long ANF time delays (in addition to the eOAE phase-gradient delays) observed in the frog, which do not appear to be associated with mechanical tuning. The frog has the smallest Q_{10} values of all the non-human species tested in the present study.

Appendix - Anatomical overview

This section provides background on the anatomy and physiology of peripheral auditory structures potentially relevant to OAE generation.

All the species examined here have a tympanic membrane enclosing the middle ear, although the presence of a tympanic membrane is unnecessary for the detection of DPOAEs (van Dijk et al. 2002). In contrast to mammals, the middle ear in the non-mammalian species examined here consists of a single bone, the columella, that couples the tympanic membrane directly to the stapedial footplate. The middle ears of both mammals and non-mammals play similar functional roles, providing both forward (stimulus going in) and reverse (OAE coming out) transmission to and from the inner ear.

The greatest amount of diversity across the examined species lies in the inner-ear anatomy (Fig. 9)[13]. Analogous to the organ of Corti in the mammalian cochlea, bird and lizard hair cells are situated in a structure called the *basilar papilla* (BP). The frog has two morphologically distinct auditory papilla in the inner ear. Specifics of the inner ear structures of each species are summarized below. The main qualitative differences in inner ear anatomy and physiology are summarized in Table I. For brevity, we provide only brief descriptions of human cochlear anatomy and hearing perception (see Dallos et al. 1996). The term "cochlea" is reserved here for the auditory organ of the mammalian inner ear.

Humans

The human cochlea (i.e. BM length) is typically 33–35 mm in length (coiled over two and a half turns) and contains around 15000 total hair cells (Ulehlova et al. 1987). Typical thresholds in a healthy human ear are relatively flat between 0.5 and 7 kHz, being in the range of -5 to 15 dB SPL. Peak sensitivity occurs in the frequency range of 3–4 kHz. Psychophysical human Q_{ERB} values typically range from 7–10 around 1 kHz to 9–17 around 4 kHz (e.g., Glasberg and Moore 2000; Shera et al. 2002)[14].

Chickens

Chickens have a short BM ($\sim$3–4 mm) that curves gently over its length. The BM width and thickness change along its length (as well as hair-cell bundle properties such as height and number of stereocilia), correlating to the tonotopic gradient observed from ANF responses (Manley et al. 1987; Chen et al. 1994). Evidence from avian species suggests that a longitudinally traveling wave

[13]Further notes with regard to Fig. 9. For the frog, the entire longitudinal length of only the amphibian papilla (AP) is shown and arrows indicate gross trends of the hair cells (the finely dashed bounding box corresponds to where the cross-section would lay and the coarsely dashed line represents where the sensing membrane extends down from the roof of the recess). Cells known to exhibit cell body somatic motility are indicated by a star on their tail. White regions are fluid-filled, grey regions correspond to overlying tectorium (with grey lines indicating fibrillar structure), grey striped area represents bone and stippled areas are non-stereociliary cellular regions (e.g., supporting cells). Distinction between scala vestibuli and scala media is omitted. Legend is as follows: AP- amphibian papilla, AR- amphibian recess, BM- basilar membrane, BP- basilar papilla, FN- fundus, LL- limbic lip, SA- sallet, SC- sallet chain, SE- sensing membrane, SM- scala media, ST- scala tympani, TC- tunnel of Corti, TM- tectorial membrane.

[14]Shera and Guinan (2003) provide a discussion on the connection between Q_{ERB} (equivalent rectangular bandwidth) and Q_{10} (in their footnote 6).

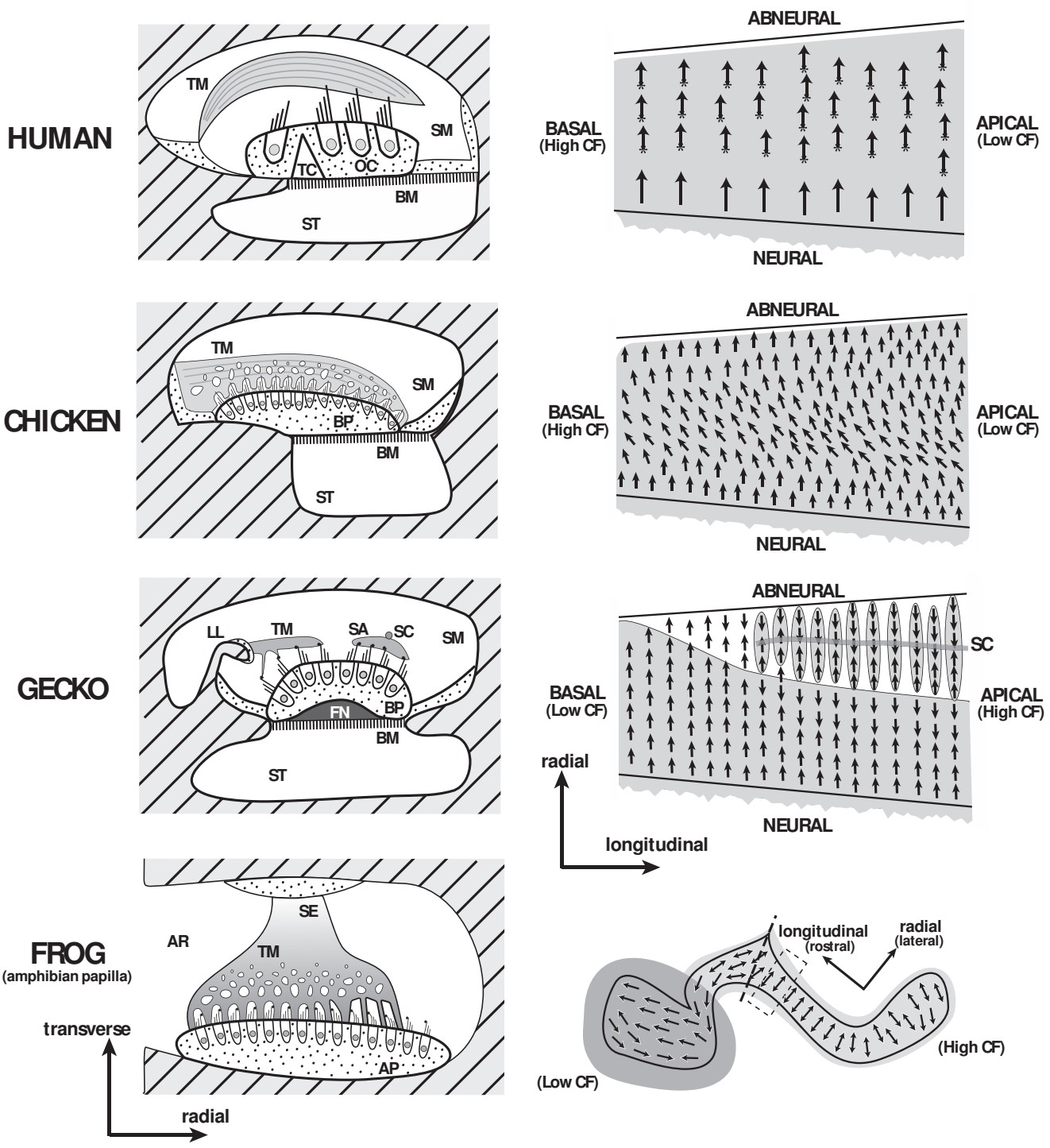

Figure 9: Comparative schematic of inner-ear anatomy. Two perspectives are provided for each group: a cross-sectional view (left) and a top-down view of a section of the sensory epithelium (right). Except for the frog, the arrows in the top-down view represent an individual hair cell, the direction indicating the bundle's polarization (pointing from shortest to tallest row). See appendix footnote for further description of figure.

is present along the BM (von Bekesy 1960; Gummer et al. 1987). There are ≈ 5000 hair cells situated in a hexagonal fashion (Tilney and Saunders 1983). In general, two distinct types of hair cells have been characterized: short hair cells sitting directly atop the BM (receiving the bulk of the efferent innervation) and tall hair cells (with the bulk of the afferent innervation) (Tanaka and Smith 1978). Chick hair cells do not exhibit somatic motility (He et al 2003; Köppl et al. 2004). The overlying TM is relatively quite thick, with dense radial and longitudinal fibers apparent under a light microscope. Cavities that are present in the TM over each hair cell extend back towards the homogene cells (at the neural edge), making the TM appear porous through a given cross-section (Cotanche 1987). For all hair cells in the papilla, the tallest row of the stereociliary bundle is tightly coupled to the TM, which is also attached to the papillar surface via fibrillar connections coupling to the microvilli of the supporting cells (Tanaka and Smith 1975).

Based upon ANF recordings from previous studies, P21 (number of days post-hatching) chicks have a flat mean threshold of ≈ 20 dB SPL from 0.2–3 kHz, increasing sharply at higher frequencies (Manley 1990). Psychoacoustic studies in adult chickens correlate well to these measurements (Saunders and Salvi 1993). Q_{10} values from the single units are typically around 2–5 (though some units exhibit significantly higher Q values), and increase with characteristic frequency (Salvi et al. 1992). While DPOAEs have been measured in the chicken (Kettembeil et al. 1995; Ipakchi et al. 2005; Lichtenhan et al. 2005), the authors know of no published reports of spontaneous emissions (SOAEs) or SFOAEs in *Gallus gallus domesticus*.

Geckos

Two species of gecko were examined in this study: Leopard geckos (*Eublepharis macularius*) and Tokay geckos (*Gekko gecko*). Both have similar peripheral auditory anatomy (Wever 1978), including a short (1.2–1.8 mm) and straight BM. Both the width and thickness of the BM and BP vary considerably over the longitudinal length. The BP contains ≈1000–2000 hair cells (Wever 1978). The BM in *G. gecko* is slightly longer and supports $\approx 40\%$ more hair cells. Hair-cell bundles are oriented both uni-directionally (all in the same direction) and bi-directionally (180° relative to one another). There is a unique tectorial topology along one region of the papilla that consists of sallets, discretized sections of TM loosely coupled to each other via a fine strand overlying their top surface called the sallet chain. The sallets couple a single row of bi-directionally oriented hair cells together as shown in Fig. 9 (Wever 1978). Evidence suggests the absence of both somatic hair-cell motility (Köppl et al. 2004) and traveling waves (Peake and Ling 1980; Manley et al. 1988; Manley et al. 1999) along the gecko BM. A thickened tissue called the fundus runs along the length of the BM underneath the BP. Both afferent and efferent innervations are present, though the latter appears exclusive to the uni-directional segment of the papilla (Manley 1990).

Previous studies have looked at microphonic responses in both species (Wever 1978) and ANF responses in *G. gecko* (Eatock et al. 1981; Sams-Dodd and Capranica 1994; Manley et al 1999), giving an indication of the thresholds and sharpness of tuning[15]. Based upon microphonic and ANF data, the *G. gecko* ear has a threshold of ≈10–15 dB SPL in its most sensitive region of 0.5–0.8 kHz. *E. macularius* appears to be a further 10–15 dB more sensitive than *G. gecko* based upon

[15]The microphonic is a gross electrical responses measured at the round window with an electrode. Wever's (1978) choice of a 1 μV microphonic threshold criterion appears to correlate well with ANF-derived thresholds, at least at lower frequencies. At higher frequencies, the bi-directional orientation of the hair bundles produces BM cancellation, creating the impression of a higher threshold (Eatock et al. 1981).

microphonic comparisons, suggesting thresholds at or below 0 dB SPL. Derived Q_{10} values from the ANF studies for *G. gecko* were ∼2–4, increasing with characteristic frequency. Spontaneous emissions have been reported in both *E. macularius* and *G. gecko* (Manley et al. 1996, Stewart and Hudspeth 2000), but the present authors are unaware of any previous reports of evoked emissions in either gecko species.

Frogs

Frogs have two papillae that are sensitive to sound, the amphibian papilla (AP) and the basilar papilla (BP) (Wever 1985). In contrast to chicks and geckos, both papillae in frogs lack a flexible BM altogether, and the hair cells sit atop relatively rigid tissue (Wever 1973). Unlike those of the human and chicken, the hair cells in the papillae do not exhibit any obvious morphological distinctions (such as short versus tall hair cells), but do exhibit a degree of bi-directionality (similar to that seen in the gecko). Shaped roughly like a horseshoe and ∼0.5–0.6 mm long (Wever 1973), the AP is tonotopically organized (Lewis et al. 1982) and is sensitive to frequencies below ∼1.2 kHz. Containing ≈ 800 hair cells, the AP has a thick TM punctuated by many small holes (Wever 1973). The hair cells couple tightly to the TM. A tectorial curtain (or *sensing membrane* extends from the bony roof of the AP recess down to the central portion of the TM. There does not appear to be a smooth gradation in either bundle or TM properties along the length of the AP (Shofner and Feng 1983; Lewis and Leverenz 1983). The BP, sensitive to higher frequencies (above ≈1.3 kHz) is smaller, containing only about 70 hair cells. The BP is thought to act as a singly tuned resonator (Ronken 1991). Unlike the AP, the BP does not appear to receive any efferent innervation in ranid frogs (Ronken 1991), though efferent innervation to the BP has been found in other amphibian species (Hellmann and Fritzsch 1996). Similar to lizards, a great deal of diversity is seen in the inner ear anatomy across different species of frogs.

Microphonic measurements in other frog species of the same family examined here indicate airborne thresholds near ∼20-40 dB SPL, being smallest in the range 0.2–0.6 kHz (Wever 1985). ANF responses in *L. pipiens* revealed higher mean thresholds, typically 50 dB SPL around 0.5–1 kHz and increasing at both lower and higher frequencies (Ronken 1991). Q_{10} values range between 1–2, increasing at frequencies below 0.5 kHz and above 2 kHz (Ronken 1991). The existence of SOAEs has been reported for *Lithobates pipiens* (van Dijk et al. 1996) while both DPOAEs (Meenderink et al. 2005) and SFOAEs (Meenderink and Narins 2006) have also been reported.

	Human	Chicken	Gecko	Frog
Overlying tectorial membrane	+	+	+	+
Flexible basilar membrane	+	+	+	−
Basilar membrane traveling wave	+	+	−	−
Hair cell somatic motility	+	−	−	−

Table II: Interspecies comparison of a few anatomical and physiological structures/properties believed relevant to OAE generation. + indicates the feature is present while − indicates its absence.

Acknowledgments

The authors acknowledge valuable discussions and comments from AJ Aranyosi, Paul Fahey, John Guinan, and John Rosowski. Comments from two anonymous reviewers are also gratefully acknowledged. This work was supported by NIH grants T32 DC00038 (CB), R01 DC000238 (DMF), R01 DC000710 (JCS), and R01 DC003687 (CAS). The experiments involving animals comply with the "Principles of animal care," publication No. 86-23, revised 1985 of the National Institute of Health and with the current laws of the United States. Experiments involving humans were carried out with the approval of the Massachusetts Institute of Technology Committee On the Use of Humans as Experimental Subjects and the Human Studies Committee at the Massachusetts Eye and Ear Infirmary.

List of Abbreviations

τ_{OAE} emission phase-gradient delay

ANF auditory nerve fiber

AP amphibian papilla

BM basilar membrane

BP basilar papilla

DPOAE distortion-product otoacoustic emission

eOAE evoked otoacoustic emission

Q quality factor

SFOAE stimulus-frequency otoacoustic emission

SOAE spontaneous otoacoustic emission

TM tectorial membrane

References

Aranyosi AJ, Freeman DM (2004) Sound-induced motions of individual cochlear hair bundles. Biophys J 87(5): 3536-3546

Boyev KP, Liberman MC, Brown MC (2002) Effects of anesthesia on efferent-mediated adaptation of the DPOAE. J Assoc Res Otolaryngol 3(3): 362-373

Brass D, Kemp DT (1993) Suppression of stimulus frequency otoacoustic emissions. J Acoust Soc Am 93(2): 920-939

Brown AM and Kemp DT (1983) An integrated view of cochlear mechanical nonlinearities observable from the ear canal. In: deBoer E and Viergever MA (eds) Mechanics of hearing. Martinus Nijhoff, The Hague, pp 75-82

Brownell WE, Bader CR, Bertrand D, Ribaupierre YD (1985) Evoked mechanical responses of isolated cochlear outer hair cells. Science 227: 194-96

Chen L, Salvi R, Shero M (1994) Cochlear frequency-place map in adult chickens: Intracellular biocytin labeling. Hear Res 81(1): 130-136

Coro F, Kössl M (1998) Distortion-product otoacoustic emissions from the tympanic organ in two noctuoid moths. J Comp Physiol A 183: 525-531

Coro F, Kössl M (2001) Components of the 2f1-f2 distortion-product otoacoustic emission in a moth. Hear Res 162: 126-133

Cotanche DA (1987) Regeneration of the tectorial membrane in the chick cochlea following severe acoustic trauma. Hear Res 30: 197-206

Dallos P, Popper AN, Fay RR (Eds.) (1996) The cochlea. New York:Springer-Verlag

Eatock RA, Manley GA, Pawson L (1981) Auditory nerve fiber activity in the gecko. I. Implications for cochlear processing. J Comp Physiol A 142: 203-218

Ferber-Viart C, Savourey G, Garcia C, Duclaux R, Bittel J, Collet L (1995) Influence of hyperthermia on cochlear micromechanical properties in humans. Hear Res 91(1-2): 202-207

Frost DR, Grant T, Faivovich J, Bain RH, Haas A, Haddad CFB, de S RO, Channing A, Wilkinson M, Donnellan SC, Raxworthy CJ, Campbell JA, Blotto BL, Moler P, Drewes RC, Nussbaum RA, Lynch JD, Green DM, Wheeler WC (2006) The amphibian tree of life. B Am Mus Nat Hist 297: 1-370

Ghaffari R, Aranyosi AJ, Freeman DM (2007) Longitudinally propagating traveling waves of the mammalian tectorial membrane. Proc Natl Acad Sci 104(42): 16510-16515

Glasberg BR, Moore BC (2000) Frequency selectivity as a function of level and frequency measured with uniformly exciting notched noise. J Acoust Soc Am 108(5): 2318-2328

Goodman SS, Withnell RH, Shera CA (2003) The origin of SFOAE microstructure in the guinea pig. Hear Res 183: 7-17

Gummer AW, Smolders JWT, Klinke R (1987) Basilar membrance motion in the pigeon measured with the Mössbauer technique. Hear Res 29: 63-92

He DZ, Beisel KW, Chen L, Ding DL, Jia S, Fritzsch B, Salvi R (2003) Chick hair cells do not exhibit voltage-dependent somatic motility. J Physiol 546(2): 511-520

Hellmann B, Fritzsch B (1996) Neuroanatomical and histochemical evidence for the presence of common lateral line and inner ear efferents and of efferents to the basilar papilla in a frog, *Xenopus laevis*. Brain Behav Evol 47: 185-194

Hillery CM, Narins PM (1984) Neurophysiological evidence for a traveling wave in the amphibian inner ear. Science 225: 1037-1039

Ipakchi R, Kyin T, Saunders JC (2005) Loss and recovery of sound-evoked otoacoustic emissions in young chicks following acoustic trauma. Audiol Neurootol 10(4): 209-219

Kemp DT (1986) Otoacoustic emissions, travelling waves and cochlear mechanisms. Hear Res 22: 95-104

Kennedy HJ, Evans MG, Crawford AC, Fettiplace R (2006) Depolarization of cochlear outer hair cells evokes active hair bundle motion by two mechanisms. J Neurosci 26(10): 2757-2766

Kettembeil S, Manley GA, Siegl E (1995) Distortion-product otoacoustic emissions and their anesthesia sensitivity in the European starling and the chicken. Hear Res 86: 47-62

Knight RD, Kemp DT (2000) Indications of different distortion product otoacoustic emission mechanisms from a detailed f_1, f_2 area study. J Acoust Soc Am 107(1): 457-473

Köppl C (1995) Otoacoustic emissions as an indicator for active cochlear mechanics: A primitive property of vertebrate auditory organs. In: Manley GA et al. (eds) Advances in hearing research. World Scientific, Singapore, pp 207-218

Köppl C, Forge A, Manley GA (2004) Low density of membrane particles in auditory hair cells of lizards and birds suggests an absence of somatic motility. J Comp Neurol 479(2): 149-155

Kössl M, Boyan GS (1998) Acoustic distortion products from the ear of a grasshopper. J Acoust Soc Am 104(1): 326-335

Lewis ER, Leverenz EL, Koyama H (1982) The tonotopic organization of the bullfrog amphibian papilla, an auditory organ lacking a basilar membrane. J Comp Physiol A 145: 437-445

Lewis ER, Leverenz EL (1983) Morphological basis for tonotopy in the anuran amphibian papilla. Scan Electron Microsc 1: 189-200

Liberman MC, Zuo J, Guinan JJ (2004) Otoacoustic emissions without somatic motility: Can stereocilia mechanics drive the mammalian cochlea?. J Acoust Soc Am 116(3): 1649-1655

Lichtenhan JT, Chertoff ME, Smittkamp SE, Durham D, Girod DA (2005) Predicting severity of cochlear hair cell damage in adult chickens using DPOAE input-output functions. Hear Res 201(1-2): 109-120

Long GR, Talmadge CL (2007) DPOAE fine structure changes at higher stimulus levels- Evidence for a nonlinear reflection component. In: Nuttall AL et al. (eds) Auditory mechanisms: processes and models. World Scientific, Singapore, pp 287-293

Manley GA, Brix J, Kaiser A (1987) Developmental stability of the tonotopic organization of the chick's basilar papilla. Science 237: 655-656

Manley GA, Yates GK, Köppl C (1988) Auditory peripheral tuning: evidence for a simple resonance phenomenon in the lizard *Tiliqua*. Hear Res 33: 181-190

Manley GA (1990) Peripheral hearing mechanisms in reptiles and birds. Springer-Verlag, Berlin

Manley GA, Köppl C, Johnstone BM (1993) Distortion-product otoacoustic emissions in the bobtail lizard. I: General characteristics. J Acoust Soc Am 93(5): 2820-2833

Manley GA, Köppl C (1994) Spontaneous otoacoustic emissions in the bobtail lizard. III: temperature effects. Hear Res 72(1-2): 171-180

Manley GA, Gallo L, Köppl C (1996) Spontaneous otoacoustic emissions in two gecko species, *Gekko gecko* and *Eublepharis macularius*. J Acoust Soc Am 99(3): 1588-1603

Manley GA, Köppl C, Sneary M (1999) Reversed tonotopic map of the basilar papilla in *Gekko gecko*. Hear Res 131(1-2): 107-116

Martin GK, Stagner BB, Jassir D, Telischi FF, Lonsbury-Martin BL. (1999) Suppression and enhancement of distortion-product otoacoustic emissions by interference tones above f(2). I. Basic findings in rabbits. Hear Res 136(1-2): 105-123

Meenderink SW, van Dijk P (2004) Level dependence of distortion product otoacoustic emissions in the leopard frog, *Rana pipiens pipiens*. Hear Res 192: 107-118

Meenderink SW, van Dijk P, Narins PM (2005) Detailed f_1, f_2 area study of distortion product otoacoustic emissions in the frog. J Assoc Res Otolaryngol 6: 37-47

Meenderink SW (2005) Distortion product otoacoustic emissions from the anuran ear. PhD Thesis, University of Maastricht.

Meenderink SW, van Dijk P(2006) Temperature dependence of anuran distortion product otoacoustic emissions. J Assoc Res Otolaryngol 7(3): 246-252

Meenderink SW, Narins PM (2006) Stimulus frequency otoacoustic emissions in the Northern leopard frog, *Rana pipiens pipiens*: Implications for inner ear mechanics. Hear Res 220(1-2): 67-75

Neely ST, Kim DO (1983) An active cochlear model showing sharp tuning and high selectivity. Hear Res 9(2): 123-130

Peake PT and Ling A Jr (1980) Basilar-membrane motion in the alligator lizard: its relation to tonotopic organization and frequency selectivity. J Acoust Soc Am 67(5): 1736-1745

Ronken DA (1991) Spike discharge properties that are related to the characteristic frequency of single units in the frog auditory nerve. J Acoust Soc Am 90(5): 2428-2440

Rosowski JJ, Peake WT, White JR (1984) Cochlear nonlinearities inferred from two-tone distortion products in the ear canal of the alligator lizard. Hear Res 13(2): 141-158

Salvi RJ, Saunders SS, Powers NL, Boettcher FA (1992) Discharge patterns of the cochlear ganglion neurons in the chicken. J Comp Physiol A 170: 227-241

Sams-Dodd F, Capranica RR (1994) Representation of acoustic signals in the eighth nerve of the Tokay gecko: I. Pure tones. Hear Res 76: 16-30

Saunders SS, Salvi RJ (1993) Psychoacoustics of normal adult chickens: Thresholds and temporal integration. J Acoust Soc Am 94(1): 83-90

Schairer KS, Ellison JC, Fitzpatrick D, Keefe DH (2006) Use of stimulus-frequency otoacoustic emission latency and level to investigate cochlear mechanics in human ears. J Acoust Soc Am 120(2): 901-914

Shera CA, Guinan JJ Jr. (1999) Evoked otoacoustic emissions arise by two fundamentally different mechanisms: a taxonomy for mammalian OAEs. J Acoust Soc Am 105(2): 782798

Shera CA, Guinan JJ Jr., Oxenham AJ (2002) Revised estimates of human cochlear tuning from otoacoustic and behavioral measurements. Proc Natl Acad Sci 99(5): 3318-3323

Shera CA, Guinan JJ Jr. (2003) Stimulus-frequency-emission group delay: a test of coherent reflection filtering and a window on cochlear tuning. J Acoust Soc Am 113(5): 2762-2772

Shera CA (2003) Wave interference in the generation of reflection- and distortion-source emissions. In: Gummer AW et al. (eds) Biophysics of the cochlea: from molecules to models. World Scientific, Singapore, pp 439-453

Shera CA, Guinan JJ Jr. (2007) Cochlear traveling-wave amplification, suppression, and beamforming probed using noninvasive calibration of intracochlear distortion sources. J Acoust Soc Am 121(2): 1003-1016

Shofner WP, Feng AS (1983) A quantitative light microscopic study of the bullfrog amphibian papilla tectorium: Correlation with tonotopic organization. Hear Res 11: 103-116

Stewart CE, Hudspeth AJ (2000) Effects of salicylates and aminoglycosides on spontaneous otoacoustic emissions in the Tokay gecko. Proc Natl Acad Sci 97(1): 454-459

Talmadge CL, Tubis A, Long GR, Piskorski P (1998) Modeling otoacoustic emission and hearing threshold fine structures. J Acoust Soc Am 104(3): 1517-1543

Talmadge CL, Tubis A, Long GR, Tong C (2000) Modeling the combined effects of basilar membrane nonlinearity and roughness on stimulus frequency otoacoustic emission fine structure. J Acoust Soc Am 108(6): 2911-2932

Tanaka K, Smith CA (1975) Structure of the avian tectorial membrane. Ann Otol Rhinol Laryngol 84(3 pt. 1): 287-296

Tanaka K, Smith CA (1978) Structure of the chicken's inner ear: SEM and TEM study. Am J Anat 153(2): 251-271

Taschenberger G, Manley GA (1997) Spontaneous otoacoustic emissions in the barn owl. Hear Res 110: 61-76

Tilney LG and Saunders JC (1983) Actin filaments, stereocilia, and hair cells of the bird cochlea. I. Length, number, width, and distribution of stereocilia of each hair cell are related to the position of the hair cell on the cochlea. J Cell Biol 96(3): 807-821

Ulehlova L, Voldrich L, Janisch R (1987) Correlative study of sensory cell density and cochlear length in humans. Hear Res 28: 149-151

van der Heijden M, Joris PX (2006) Panoramic measurements of the apex of the cochlea. J Neurosci 26(44): 11462-11473

van Dijk P, Narins PM, Wang J (1996) Spontaneous otoacoustic emissions in seven frog species. Hear Res 101: 102-112

van Dijk P, Mason MJ, Narins PM (2002) Distortion product otoacoustic emissions in frogs: correlation with middle and inner ear properties. Hear Res 173: 100-108

van Dijk P, Narins PM, Mason MJ (2003) Physiological vulnerability of distortion product otoacoustic emissions from the amphibian ear. J Acoust Soc Am 114(4): 2044-2048

von Bekesy G (1960) Experiments in hearing. New York:McGraw-Hill

Veuillet E, Gartner M, Champsaur G, Neidecker J, Collet L (1997) Effects of hypothermia on cochlear micromechanical properties in humans. J Neurol Sci 145(1): 69-76

Werner YL (1976) Optimal temperatures for inner-ear performance in gekkonoid lizards. J Exp Zool 195(3): 319-352

Wever EG (1973) The ear and hearing in the frog, Rana pipiens. J Morphol 141: 461-478

Wever EG (1978) The reptile ear. Princeton University Press.

Wever EG (1985) The amphibian ear. Princeton University Press.

Whitehead ML, Stagner BB, Martin GK, Lonsbury-Marin BL (1996) Visualization of the onset of distortion product otoacoustic emissions, and measurement of their latency. J Acoust Soc Am 100(3): 1663-1679

Zweig G., Shera CA (1995) The origin of periodicity in the spectrum of evoked otoacoustic emissions. J Acoust Soc Am 98(4): 2018-2047